RSC Advances

REVIEW

View Article Online
View Journal | View Issue

Cite this: *RSC Adv.*, 2025, **15**, 167

Microfluidic-based electrically driven particle manipulation techniques for biomedical applications

Jiulin Wang,[a] Xinyuan Cui,[b] Wei Wang,[a] Junhao Wang,[a] Quili Zhang,[c] Xiaonan Guo,[c] Yanfeng Liang,[c] Shujin Lin,*[a] Bingfeng Chu*[d] and Daxiang Cui*[ac]

Received 1st August 2024
Accepted 29th September 2024

DOI: 10.1039/d4ra05571c

rsc.li/rsc-advances

Microfluidic chips exhibit unique advantages in both economy and rapidity, particularly for the separation and detection of biomolecules. In this review, we first introduced the mechanisms of several electrically driven methods, such as electrophoresis, dielectrophoresis, electro-wetting and electro-rotation. We then discussed in detail the application of these methods in nucleic acid analysis, protein manipulation and cell treatment. In addition, we outlined the considerations for material selection, manufacturing processes and structural design of microfluidic chips based on electrically driven mechanisms.

1. Introduction

Microfluidic chip technology stands at the forefront of the micro total analysis system, representing an innovative field that intersects various disciplines.[1,2] The sampling, separation, and detection systems are seamlessly integrated onto glass, quartz, silicon, or polymer wafers to create microfluidic chips.[3] They are widely used in many domains, including DNA analysis,[4] protein separation,[5] cell biology,[6,7] and medical diagnostics.[8] This all-encompassing approach has found new applications in tissue engineering,[9] drug screening,[10] biomolecular identification,[11] and single-cell[12] and stem-cell function analysis.[13]

A variety of microfluidic devices have been used for particle separation. Active microfluidic devices harness various external forces, such as magnetic, electric, acoustic, centrifugal, and optical trapping forces, endowing the systems with remarkable versatility.[12] For example, optical methods provide accurate manipulation of individual particles but rely on precise optical systems and manual operation. Utilizing sound waves for the classification necessitates certain piezoelectric actuators and flow channel configurations.[14] In magnetic drive, a weak magnetic field will cause problems in the interaction between the surface and the interior of the chip.[15] The electrically driven technique addresses the limitations of the aforementioned methods and serves as a fundamental approach for characterizing and manipulating particles. Electrokinetic operations can be categorized into electrophoresis, dielectrophoresis, electroosmosis, electrorotation and so on. This review is organized mainly based on this classification. Dielectrophoretic techniques are used to manipulate uncharged particles, while electrophoresis or electroosmosis controls the mobility of charged particles.[16] The difference between dielectrophoresis and electrophoresis is whether they work on the induced or fixed charges of the particles, respectively. Dielectrophoresis is used to manipulate, separate, and characterize biological particles,[17] while electroosmosis makes it easier for nanoscale biological particles to move within tiny microfluidic chips, and electrorotation is commonly employed for the characterization of micron-scale biological cells.[18] This review focuses on electrically driven mechanisms and biological applications, including electrophoresis, dielectrophoresis, electroosmosis, electrowetting-on-dielectric, and electrorotation(as shown in Fig. 1).

2. Advances of microfluidic-based electrophoresis drive mode

Electrophoresis refers to the movement of charged surfaces and their attached substances relative to a stationary liquid under the influence of an external electric field. This motion is brought about by the Coulomb force that the particles experience as a result of their surface charges.[19]

The combination of electrophoresis and microfluidic chip is applied to the detection of biomarkers.[20,21] Many detection modes, such as laser-induced fluorescence (LIF), ultraviolet

[a]*Institute of Nano Biomedicine and Engineering, School of Sensing Science and Engineering, School of Electronic Information and Electrical Engineering, Shanghai JiaoTong University, Shanghai 200240, PR China. E-mail: aaron.lin@sjtu.edu.cn; dxcui@sjtu.edu.cn*

[b]*Department of Radiology, Ruijin Hospital, Shanghai Jiao Tong University School of Medicine, Shanghai, 200025, PR China*

[c]*First Affiliated Hospital, Henan University School of Medicine, Kaifeng 475000, PR China*

[d]*Department of Stomatology, The First Medical Centre, Chinese PLA General Hospital, Beijing 100853, PR China. E-mail: chubingf@aliyun.com*

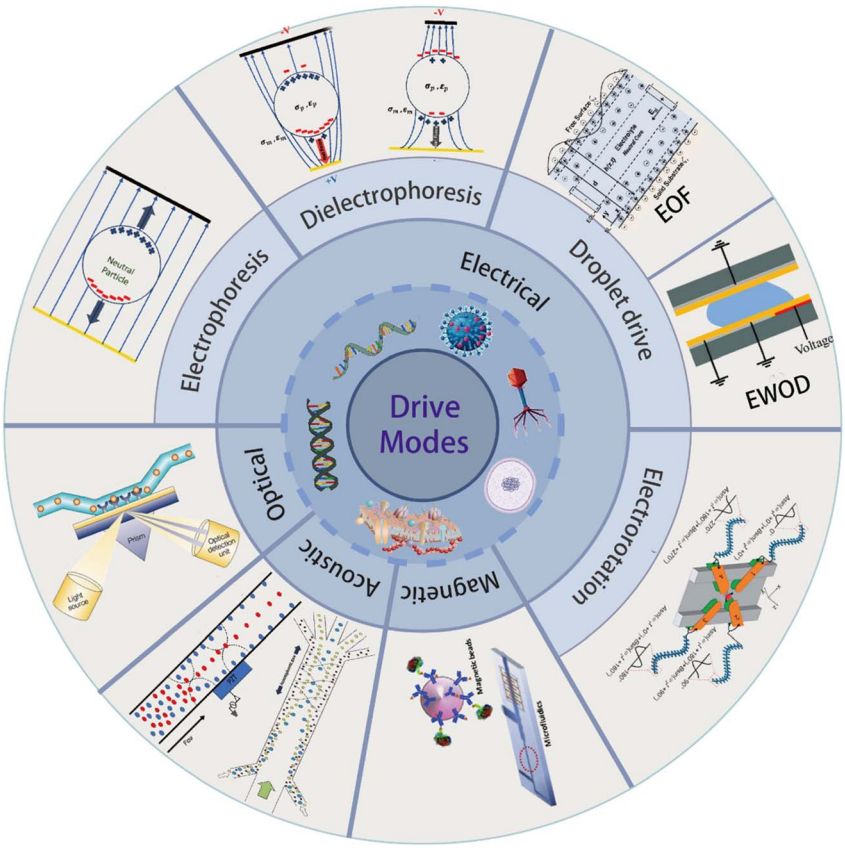

Fig. 1 An overview of the biological particle microfluidic drive techniques. The driving force of microfluidic techniques can be further subdivided into optical, acoustic, magnetic, and electrical forces. EOF: electroosmotic flow; EWOD: electrowetting-on-dielectric.

(UV), and mass spectrometry (MS), as well as capillary zone electrophoresis (CZE), capillary gel electrophoresis (CGE), isotachophoresis (ITP), micellar electrokinetic chromatography (MEKC), and isoelectric focusing (IEF), are based on microfluidic electrophoresis technology and have been used for the separation and analysis of various samples.[22] The subsequent discussion presents several representative electrophoretic techniques, each generating an electric field through distinct mechanisms. A key feature of zone electrophoresis (ZE) is the lack of solid support, which enhances the recovery rates and allows active sample compounds to run continuously, boosting sample throughput. ZE is distinguished by a high rate of biological activity recovery and separation efficiency, even when it comes to purify proteins from complicated protein extracts.[23] In contact charge electrophoresis (CCEP), conductive particles and droplets oscillate between two or more electrodes with the help

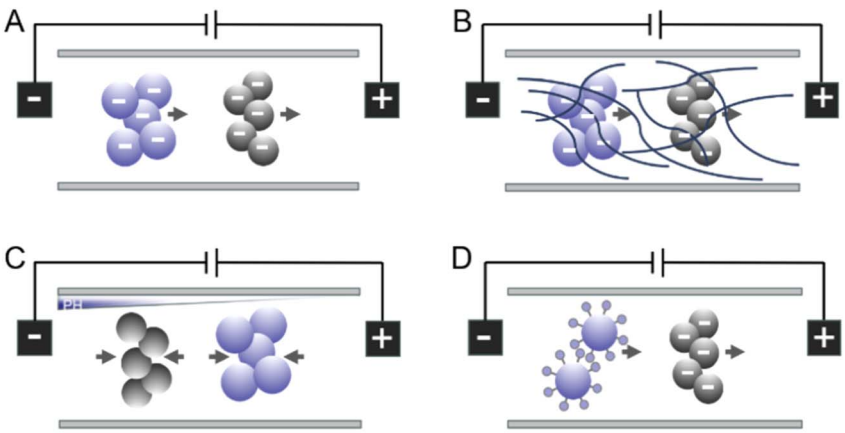

Fig. 2 Electrophoresis modes used in microsystems: (A) free solution electrophoresis. (B) Gel electrophoresis. (C) Isoelectric focusing. (D) Micellar electrokinetic chromatography (with negatively charged analytes depicted).[25]

of a steady electric field. In contrast to conventional electrophoretic methods, constant and quick particle motion powered by low-power direct current voltage is possible with CCEP.[24] Free solution electrophoresis is a method that separates molecule analytes based on the speed at which they move in response to an applied electric field. Surface charge and buffer pH should be carefully regulated to achieve optimal separation performance. Some of the basic principles of the electrophoresis models are depicted in Fig. 2.[25]

2.1 Capillary electrophoresis

The separating medium employed in Capillary Electrophoresis (CE) is a fused silica capillary, which distinguishes it from other electrophoretic techniques. Because of its high separation efficiency, minimal reagent and sample consumption, and quick analysis time, CE is a frequently used analytical technique that has evolved into a potent microanalytical platform in biology and medicine.[26] Additionally, CE is compatible with many detection methods such as absorbance, laser-induced fluorescence, mass spectrometry, and voltammetry. It is widely used to control buffer flow and manipulate sample solutes, such as sample injection, separation, mixing, dilution/concentration, and reaction. CE is now widely used for the separation of various analytes, ranging from tiny ions to big proteins and DNA fragments, owing to its high throughput. Typical applications include fragment size estimation, SSCP or RFLP analysis,[27] and DNA sequencing.[28]

However, the process of manipulating sample separation in CE is associated with certain defects. There are a number of difficulties with protein separation using CE, including protein adsorption on the capillary wall, coating stability, and lack of electroosmotic flow (EOF) control. Protein and capillary electrostatic interaction results in the imperfection of protein adsorption on the channel wall. This adsorption will contaminate the surface of the channel wall, resulting in an uneven potential in the separation chamber and ultimately peak asymmetry or band widening. Protein adsorption thus causes short migration duration, lower detection response, poor reproducibility,[29] reduced resolution and decreased separation efficiency. In an additional instance, ion mobility in CE is also influenced by another process called EOF. Non-reproducible electroosmotic flow (EOF) may affect the resolution and repeatability of separated proteins. Reducing EOF helps improve protein resolution because if the coating produces a large amount of EOF, the protein will migrate out of the capillary before it reaches the resolution.[30]

Thus, in order to reduce the non-specific adherence of protein, the surface needs to be treated.[31] Due to the extremely high surface-to-volume ratio in microchannels and nanochannels, any molecules that stick to the surface may block the channel. Additionally, it is critical to note that the inherent hydrophobicity of the PDMS material increases the likelihood of biological samples interacting with the material surface in a biological environment. Therefore, numerous capillary surface modifications have been developed to prevent adsorption and provide effective and repeatable electrophoretic separation.[32] Numerous strategies have been devised by researchers to address the issue of protein adsorption; however, none of them are universally effective. For example, Y. Liang *et al.*[33] used trypsin photopolymerization and covalent binding to synthesize a new hydrophilic monomer copolymer. Its great hydrophilicity aids in reducing peptide overlap, preventing sample cross-contamination, and preventing non-specific protein and peptide adsorption. It also shows tremendous promise for high-throughput proteomic analysis. With a two-dimensional MCE device, R. Wu *et al.*[34] used a multidimensional approach to improve the resolution of the significant minor proteins by separating the major proteins in the chip. A portable genetic analysis microsystem for pathogen identification using integrated polymerase chain reaction (PCR) and sliding valveless capillary electrophoresis (CE) has been created.[35] PEG can be applied to the surface to stop non-specific protein adsorption. Alkyne-PEG was covalently bonded to the azide-PDMS surface after alkyne-PEG was created using standard synthetic methods.[36] EOF measurements demonstrated a 30 days maximum suppression of EOF in modified PDMS microchannels.

Because CE is particularly advantageous at separating DNA, it is frequently employed in biological applications involving DNA. Because capillary electrophoresis has no moving components, pulse-free pumping, and can separate small sample quantities quickly, it has been effectively employed for measuring DNA.[37] Common CE chip layouts for separating and detecting DNA/RNA are shown in Fig. 3A.[38] DNA has a high charge density, which is lessened on the backbone by manning condensation in some counterions. When DNA dissolves in solution, it has a negative charge since it is an acid (Fig. 3B).[39] The effective breadth of the DNA skeleton is altered in solutions due to electrostatic interactions. When two sections of DNA get closer together, the electrostatic repulsion caused by their overlapping double layers makes them appear thicker than their bare width.[41] Usually, the material or higher Joule heating limits the applied voltage.[42] The separation length on microfabricated devices with limited area can be enhanced by winding curved channels. Sharp bends, furthermore, result in dispersion and bandwidth, which are governed by the superposition of field strengths inside and outside and the variation in inner and outer corner lengths. To address these issues, it is advisable to explore the possibility of reducing the separation length or increasing the voltage in order to minimize the analysis duration.

There are several smaller-scale development areas for DNA separation techniques based on CE. The target-binding single-stranded DNA (ssDNA) can be carried by the applied potential difference between the chambers, and J. Kim *et al.* developed a method that combines solid-phase extraction and electrophoresis to separate and enrich ssDNA from a random DNA mixture.[43] C. Heller *et al.*[44] studied the mechanism of DNA movement in a porous matrix, which helps to optimize the DNA separation in capillary electrophoresis and improve the DNA separation model in a porous matrix. Hui J. *et al.*[45] proposed that CE could be helpful in purifying minuscule quantities of DNA origami. Since the migration times of origami vary

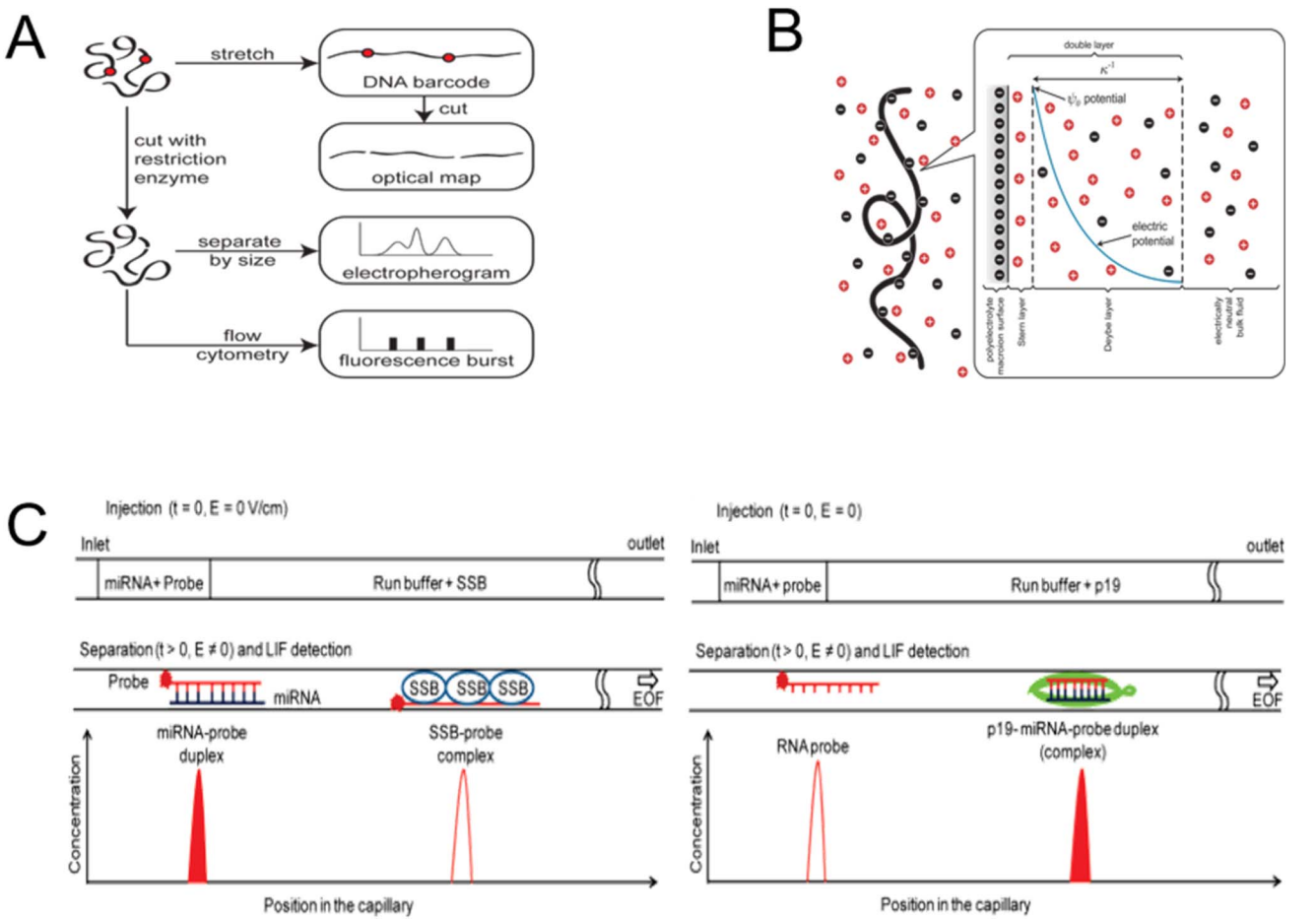

Fig. 3 Detection and separation of DNA using capillary electrophoresis. (A) The chip is made up of a chamber with inlets and a network of microchannels for CE analysis.[38] (B) Diagram of the local electrostatics in the vicinity of a free-solution DNA coil.[39] (C) The protein-facilitated affinity capillary electrophoresis (ProFACE) is used to detect miRNA.[40]

depending on their shape, CE can also be used to identify misfolded origami creations. Reducing the detection limit, shortening the analysis time, and increasing the separation efficiency are some trends of capillary electrophoresis microfluidic separation technology.

The capillary electrophoresis technique is employed not only for DNA separation but also for RNA separation. MicroRNAs (miRNAs) are a kind of short, noncoding RNAs that contain about 18–22 nucleotides.[46] MiRNA genes are considered crucial for a wide range of physiological and pathological processes. Consequently, the sensitive detection of multiple miRNAs has become critically important, as many diseases are associated with the dysregulation of several miRNAs.[47] A capillary electrophoresis technique based on hybridization between DNA probes and miRNAs was created for the direct detection of multiplex miRNAs.[48] In order to achieve multiplex detection of miRNAs using CE separation, E. Ban *et al.*[49] constructed three fluorescein amidite (FAM) and Cy5 labelled DNA probes that would bind uniquely to various target miRNAs. P. Zhang *et al.*[50] conducted a highly sensitive study of three miRNAs using ligase chain reaction (LCR) in conjunction with CE separation. Moreover, proteins may assist in miRNA detection. A tiny plug made of a miRNA and a fluorescently tagged probe is inserted into a capillary and electrophoresed. A specific virus-encoded protein only binds to the miRNA-RNA probe duplexes (Fig. 3C).[40]

In summary, CE has a major advantage over traditional approaches due to its small capillary size and perfect control over experimental settings. Compared to other electrophoretic methods, CE provides better resolution since it can reduce diffusion effects and improve repeatability.

2.2 Gel electrophoresis

Gel electrophoresis is used for compound separation, which can be carried out in capillary or slab gel form or with various forms of affinity chromatography. A gel matrix with microscopic pores is pushed through by an electrical field during the gel electrophoresis process to separate the molecules. Gel electrophoresis can lessen diffusion and widen the separation zone because the gel matrix adsorbs along the microchannel wall and neutralizes the surface charge. The two common media used in gel electrophoresis are polyacrylamide and agarose. While agarose forms a physical gel that is typically used to separate longer DNA, polyacrylamide gel is chemically crosslinked and used to

separate shorter double-stranded and single-stranded DNA.[51] Therefore, DNA fragment size can be ascertained and separated samples can be recovered.

The migration rate of DNA molecules during gel electrophoresis is influenced by numerous factors. Lee, P. Y. *et al.*[52] listed the following among the most important impacts on the rate of migration of DNA molecules through agarose gel: the size of the nucleic acid molecule studied; agarose gel concentration; nucleic acid conformation; the voltage applied; the presence of ethidium bromide; the type of agarose gel; electrophoresis buffer. Gel-based separations of nucleic acid biopolymers entail sieving mechanisms that are determined by the disparity between the gel's apparent pore size a and the size of the polymer molecules R_g.[53] The relationship between the morphology and movement mechanism of DNA molecules in gels is associated with the R_g/a ratio. For instance, Ogston sieving takes place when the DNA molecules are smaller than the gel pore size (Fig. 4A). As the DNA size approaches (Fig. 4B) or exceeds the gel pore size (Fig. 4C), it deforms by reptating or stretching through the gel. These various modes of sieving are harnessed to optimize gel-based separations, enabling the resolution of specific size ranges within a given sample.

In general, the benefit of gel electrophoresis lies in its ability to combine all processes onto a single chip, including cell sorting, cell lysis, extraction of pertinent material (such DNA), purification, separation, and analysis of DNA (Fig. 5A). Gel zones in microscale channels have even facilitated the extraction of DNA from bacteriophage[54] as well as MCF-7 (ref. 55) and SKBR3 (ref. 56) cells. In a distinct application of sieving-based DNA separations, thermally reversible self-assembled gels, specifically composed of Pluronic F127, were effortlessly patterned within microfluidic channels. This setup enabled the observation of gel-limited diffusion during electrophoretic stacking of DNA molecules. Subsequently, a size-dependent

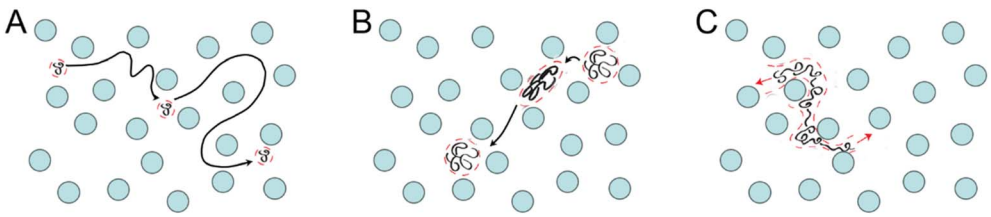

Fig. 4 DNA separation process utilizing gel electrophoresis. (A) $R_g/a \ll 1$. (B) $R_g/a \approx 1$ (C) $R_g/a \gg 1$.

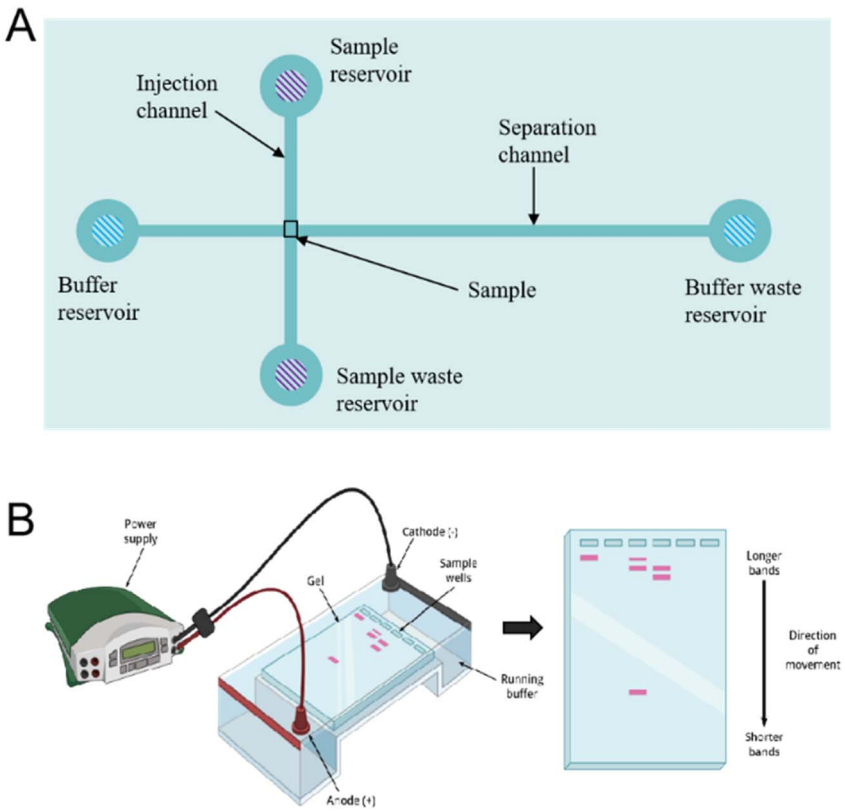

Fig. 5 Schematic of the microfluidic gel electrophoresis apparatus. (A) Typical layout of miniaturized gel electrophoresis equipment. (B) A process diagram for distinguishing DNA by gel electrophoresis.[57]

sieving process was executed, effectively separating the DNA based on molecular size[57] (Fig. 5B). Konishi, T *et al.*[58] utilized agarose gel electrophoresis to quantify DNA single-strand breaks (SSBs) and double-strand breaks (DSBs), in order to assess DNA damage in cell therapy. Similarly, Haberland, V *et al.*[59] used gel electrophoresis to assess the induction and repair of DSB by manganese.

Even with widespread use, the system still has certain built-in flaws: during the separation process, separation parameters cannot be changed or optimized; significant shear force effects can affect the integrity and function of the analytes; sample elution and post-processing can be challenging and may even require the use of toxic or mutagenic reagents;[60] the process is semi-quantitative;[61] the analysis process can be time-consuming.

2.3 Free-flow electrophoresis (FFE)

Free-flow electrophoresis (FFE), also known as carrier-free electrophoresis, is a matrix-free, high-voltage electrophoretic separation technique. A sample is introduced into the carrier electrolyte in a fluid dynamic pumping liquid system and flows through the channel in a laminar state with an electric field perpendicular to the fluid. Numerous techniques including free-flow zone electrophoresis and free-flow isoelectric focusing (Fig. 6A) have been developed for the multifunctional activity of separating DNA, cells, protein isoforms, peptides, and nanoparticles.[62]

The main benefit of FFE is that it can separate samples dissolved in a liquid solvent quickly and gently, doing away with the requirement for a matrix. Because analytes do not cling to any carrier or matrix structure, this property guarantees an extremely high recovery rate. Furthermore, native and denaturing conditions can be used for these separations. By creating a pH gradient, FFE makes it easier to quantitatively separate samples based on isoelectric point or charge variations (Fig. 6B).[63] The separation of charged particles and proteins was the main focus of FFE developments. The greater resolution in protein separation and improved particle electrophoresis capabilities of free-flow electrophoresis, according to R. Wildgruber *et al.*,[65] have made it an efficient method for preparing relevant peptide mixtures. However, the utilization of free-flow electrophoresis in comparative proteomic research is limited since protein samples must be processed sequentially rather than continuously, which raises inherent uncertainty when attempting to undertake quantitative analysis. To solve this shortcoming, the K. Y. C. Fung group introduced a technique that uses fluorescent CyDye technology and free-flow electrophoresis to simultaneously separate and identify differentially expressed proteins in a model cell system (DIGE).[66]

Furthermore, several teams are developing micro FFEs, or smaller versions of FFE systems. Micro free-flow electrophoresis systems only require tens of nanolitres to hundreds of microliters of samples, as opposed to the tens of millilitres of samples that standard large-scale FFE machines consume.[64] The

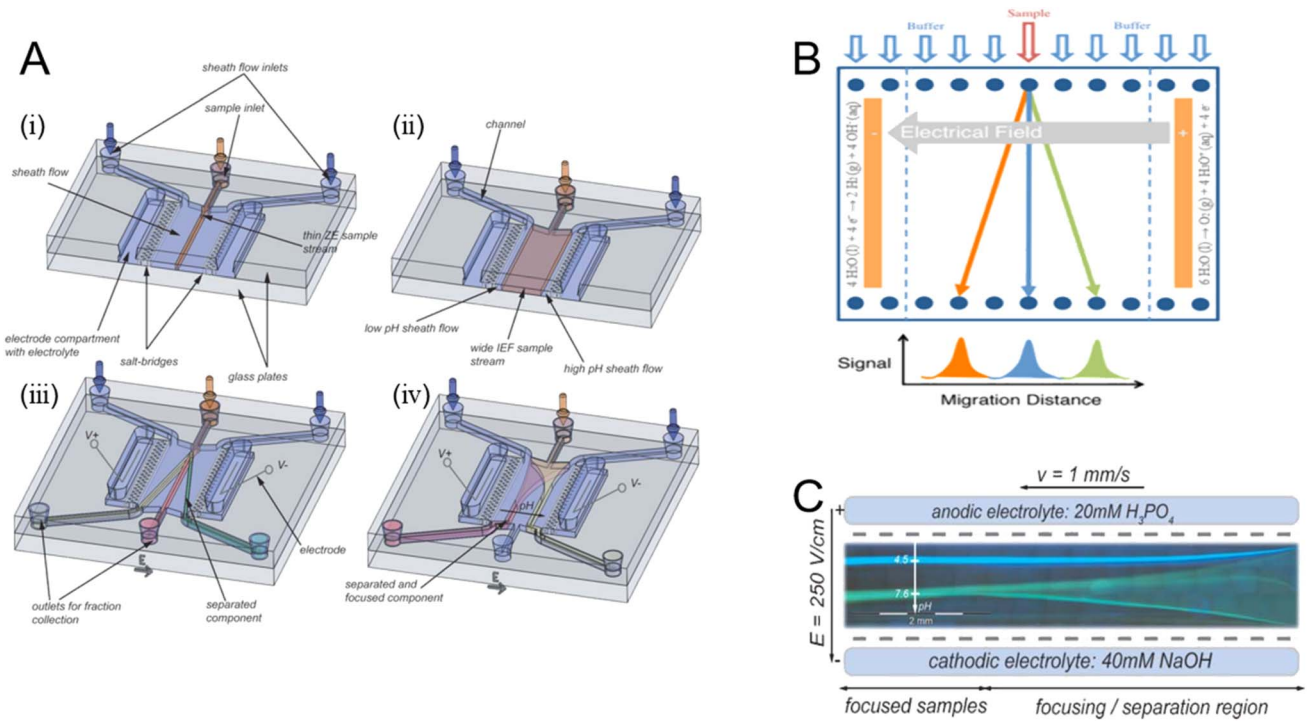

Fig. 6 (A) An illustration of the m-FFE gadget and its separation mechanisms. (i and iii) Free-flow zone electrophoresis is applied. (ii and iv) Free-flow isoelectric focusing application.[62] (B) General principle of separation in free-flow electrophoresis: the analyte's electrophoretic mobilities are used to deflect the sample stream laterally in an electric field as it is constantly supplied into the separation chamber.[63] (C) Feasibility to direct the components to particular chip outlets by hydrodynamically concentrating the sample streams between two buffer streams and altering the inlet flow ratio of the two sheath flow streams.[64]

Table 1 Summary of biological particle manipulation and separation electrophoretic techniques

Microfluidic technique	Separation medium	Particle types	Processing time	Separation mechanism	Resolution	Strengths	Limitations	Ref.
Capillary zone electrophoresis (CZE)	Capillary electrophoresis	Ions, tiny molecules	5–30 min	Size-based	90–99%	Quick and easy preparation	Inadequate resolution for intricate mixtures	72 and 73
Capillary gel electrophoresis (CGE)	Capillary electrophoresis	Proteins, nucleic acids	30–60 min	Size-based	90–99%	High resolution, wider range of gel matrix materials	Gel matrix causes slower speed	74 and 75
Capillary isoelectric focusing (CIEF)	Capillary electrophoresis	Proteins, peptides, viruses, vesicles	30–120 min	Isoelectric point-based	95–99%	Automation of procedures and short analysis time	Time-consuming, difficult with complicated samples	76 and 77
Capillary isotachophoresis (CITP)	Capillary electrophoresis	Nucleic acids, peptides, proteins	10–30 min	Mobility-based	85–95%	Effective for complicated mixtures	Concentration effects	78–80
Micellar electrokinetic capillary chromatography (MECC)	Capillary electrophoresis	Amino acids, phenols, oligonucleotides	10–30 min	Size-based	90–99%	Adaptable, capable of separating charged and neutral compounds	Reproducibility is impacted by micelle stability	81 and 82
Capillary electrochromatography (CEC)	Capillary electrophoresis	Liposomes, DNA or RNA, lipoproteins	10–60 min	Charge-based	90–99%	Superior resolution, appropriate for detectors	Elaborate optimization	83 and 84
Polyacrylamide gel electrophoresis (PAGE)	Gel electrophoresis	Minimal, molecular weight protein	1–4 h	Size-based	95–99%	Improved resolution following modification	Toxic monomers, more challenging than agarose gels	85 and 86
Agarose gel electrophoresis (AGE)	Gel electrophoresis	DNA with hundreds of base pairs	30–120 min	Size-based	90–99%	Fundamental functioning, versatility	Low throughput, the buffer may be exhausted	87 and 88
Isoelectric focusing (IEF)	Gel electrophoresis	Proteins, peptides	1–4 h	Isoelectric point-based	95–99%	Reduce the convection, high-efficiency	Restricted resolution, challenging detection	36 and 89
Moving boundary electrophoresis (MBE)	Free flow electrophoresis	Macromolecules	Several hours	Mobility-based	85–95%	Support media are not needed, recover biologically active molecules	Low resolution, an intricately configured optical system is necessary	90 and 91

integration of electrodes and flow control can be accomplished by combining free-flow electrophoresis with other methods in micro FFEs (Fig. 6C).[64] For example, A. Zhang *et al.*[67] proposed utilizing laser-assisted chemical etching of glass, followed by electrode integration and low-temperature bonding, to attain high throughput and high stability in a micro-free-flow electrophoresis device. S. Jezierski *et al.*[68] demonstrated a rapid and flexible technique for fabricating functional micro free-flow electrophoresis devices. These microfluidic chips have hydrophilic surfaces and ion-permeable segregation walls between the electrode channels and the separation bed. The performance of the chip is demonstrated by isolating fluorescent xanthene dyes and fluorescently tagged amino acids *via* free-flow electrophoretic separation.

Microfluidic free-flow electrophoresis offers several advantages such as reduced sample residence time, quicker separation time, cost savings, ease of portability, integration of multiple operation units, high aspect ratios that facilitate quick heat dissipation and high electric field strength settings, and enhanced laminar states in channels with micron-scale feature sizes.[69] The biological sciences greatly depend on the identification and separation of proteins, peptides, and amino acids,[70] while high-efficiency separation with little sample dilution is possible with electrophoretic injection.[71] The use of a liquid matrix affects the parallelization of separation, meaning that only one mixture/sample is separated at a time, but it also enables quick separation and direct sample collection. A summary of the analysis of several typical electrophoretic techniques is given in Table 1.[72–91]

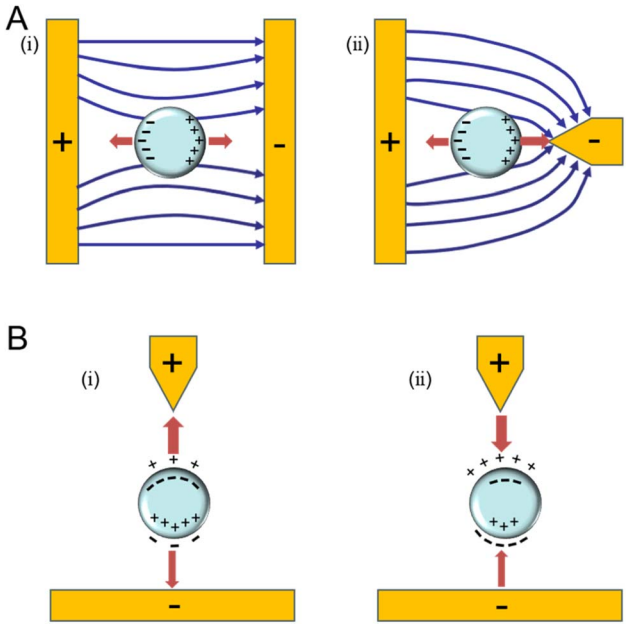

Fig. 7 Diagrams that illustrate the principle of DEP. (A) Positive dielectrophoretic (pDEP) diagram. (i) In a homogeneous electrical field, the particle is symmetrically polarized, producing a net DEP force (FDEP) with zero amplitude. (ii) The particle moves into an area with the largest amplitude of the electric field because it is asymmetrically polarized in the non-uniform electric field (NUEF) and the net FDEP.[92] (B) A non-uniform electric field causes the dielectrophoretic force to act on the induced dipole: (i) positive DEP and (ii) negative DEP.[93]

3. Advances of microfluidic-based dielectrophoresis (DEP) drive mode

When a dielectric particle is subjected to an uneven electric field, it experiences a phenomenon known as dielectrophoresis (DEP). In this non-uniform electric field, particles move due to the interaction of their respective dipoles with the spatial gradient present. Particle dipoles come from two sources: the permanent dipole, which is always present and is produced by the orientation of the atoms. The other source is the induced dipole, which results from the presence of an external electric field causing the charges on the particle surface to reorient (Fig. 7B). The frequency of the applied field dictates the exact composition of the dipoles. At lower frequencies, free charge dipoles are predominant, whereas at higher frequencies, polarized charge dipoles dominate.[92]

The particle experiences distinct forces at both ends when the particle-medium system is subjected to an uneven electric field. Depending on the rate at which the particle and the medium polarize, the difference in force at both ends will result in a net force in either direction.[94] The concept of polarization rate can be thought of as an indicator of the capacity of a substance to produce charge at the interface. An extra mechanism resulting from the build-up of charge at the interface between two distinct dielectrics is interfacial polarization. An alternative approach to polarization, known as particle polarization, is not universally applicable. The effectiveness of the interaction between the polarized particles and the electrodes is limited to the immediate vicinity of the electrodes. It is ineffective for transporting particles over great distances. The lateral dimension of the channel is within the range of this contact force when combined with microfluidic devices. The driving force that results in the separation and lateral focus of the channel is formed by the repulsive force that exists between the electrodes and the particles.[95]

In DEP, the polarized objects experience a force from the electric field gradient, which leads to either migration or capture. Particles do not necessarily need to have a surface charge in order to be polarized by an alternating current. Depending on the electroosmotic characteristics of the particles and the liquid, particles in an alternating electric field will migrate toward or away from the strongest field zone. Positive DEP, or the maximum field, attracts particles whose permeability is greater than that of the fluid; negative DEP is the opposite (Fig. 7A). By measuring the frequency of individual particles, DEP can be used to determine the electrical characteristics of the particles.[93] It is simpler to discriminate between different particles when the electrical properties of particles are measured at different frequencies.[96] In contrast to electrophoresis, DEP is capable of detecting a large number of intrinsic properties including permittivity, deformability, size,[97] shape, charge distribution, and mobility.[98] DEP may differentiate and categorize biological cells based on internal conductivity, size

variation, and membrane properties (permeability,[99] capacitance,[100] and conductivity[101]) by measuring the dielectric difference between various particles or cells.

Numerous elements will also impact the result of dielectrophoretic force. The dielectrophoretic force must be strong enough to overcome opposing forces including buoyancy, drag force, electrothermal force, alternating current electroosmotic force, and Brownian motion in order to be used to manipulate particles and cells. Several factors influence the dielectrophoretic force acting on the particles, including their charge, the shape of the device, the permittivity of the medium and the particles, and their physiological characteristics.[102] Other factors that can affect DEP include the suspending medium's electric field and molar concentration; however, their range of adjustment is constrained. In a different scenario, the cell position is mapped to the Clausius–Mossotti (CM) factor by the force balance between the DEP force and the fluid resistance, producing an observable equilibrium position.[103] With the DEP spring, which was developed by H.-W. Su *et al.*,[104] the fluid resistance balances the DEP force produced by the coplanar electrodes, creating a clear equilibrium position.

3.1 Classification of dielectrophoretic techniques

The gradient of the electric field had a significant impact on the dielectrophoretic force that caused the movement.[105] Consequently, DEP can typically be categorized into the following groups based on the type and gradient of the electric field: AC-DEP, DC-DEP, insulator-based DEP (iDEP), DC-iDEP, combined AC/DC (AC-iDEP), and traveling wave DEP (twDEP).

In AC DEP, to produce a spatially nonuniform electric field, an array of metal electrodes is often inserted inside a microdevice for AC DEP. This technology simplifies particle separation by altering the properties of the medium and adjusting the frequency of the applied electric field (Fig. 9A). Furthermore, it can counteract any electroosmotic and electrophoretic effects.[106] However, the need for external pumping to drive the particles through the device complicates its operation. DC DEP and AC DEP can both be used to separate particles based on size, but the fundamental issue with size separation with DC DEP is that it requires a significant size difference between the particles, whereas AC DEP can separate particles based on attributes.

In DC DEP, specifically engineered electrically nonconducting barriers or hurdles within a microdevice are often responsible for producing the spatially nonuniform electric field.[107] External pumping is not necessary since the DC electric field creates EOF within the system. There are various benefits to using insulating impediments to induce nonuniformities in the channel such as continuous flow inside the microdevice and streamlined device construction procedures.[108] However, this microdevice relies on a relatively high-conductivity medium for the separation of biological particles, which may make it susceptible to the negative effects of Joule heating and electrothermal flow. Compared to AC dielectrophoretic techniques, it also requires relatively high electric potentials to achieve similar electric effects.[109] The integrity of biological particles and their separation may be jeopardized by these occurrences.

The combined AC/DC DEP method makes use of both AC and DC effects: AC DEP is used for particle separation, while DC DEP uses electrokinetic effects such as electroosmosis to promote particle transport. High voltage is needed for DEP applications because the electrodes at the inlet and exit reservoirs create the electric field. Direct current or low-frequency alternating current fields are preferred because it is more feasible to generate low-frequency high alternating current voltages. Thus, the connection between the DEP force field and the flow field is determined by the voltage applied by the reservoir. This restricts the adaptability of the system and maintains voltage as the only control parameter.

Using a traveling wave DEP approach, an electric field gradient is created between two parallel electrodes by changing the phase of the applied electric field. Particle transport and separation in traveling-wave DEP are accomplished solely using the AC electric field. This technique includes phase-shifting AC voltages one after the other in order to produce spatial nonuniformity in the electric field's magnitude and phase.[110] Particle movement is driven by phase nonuniformity, and particle separation is facilitated by magnitude nonuniformity. Once the sample is inserted at its microchannel, a pressure-driven flow pulls it through the channel during the twDEP process for cell separation (Fig. 9D).[111]

Apart from dividing according to the electric field gradient, dielectrophoretic devices can also be categorized according to the designs they have. The creation of an inhomogeneous electric field that produces the dielectrophoretic force can be accomplished by two methods: either by applying a voltage to an integrated metal microelectrode array (an electrode-based DEP)[112] (Fig. 8) or by placing an insulating structure between two electrodes (an insulator-based DEP, contactless DEP).[113] The preceding examples illustrate DEP systems using electrodes, while this section focuses on DEP systems that employ insulating materials. The conductive media and channel insulators in iDEP define the electric field. Several materials have been used to fabricate microdevices that alter the electroosmotic velocity and wall surface charge, allowing for field non-uniformity regulated by the geometry of the obstacle. Researchers suggested various designs of insulating barriers including rectangular, triangular, circular, sawtooth,[114] snake-shaped channel,[115] circular column,[116] and open-top microstructure.[117] Different insulating materials can be employed in DEP.[108] An insulating structure can be positioned between the electrodes in addition to determining the shape of the insulating barrier. Examples of such structures include oil barriers,[118] membrane pores,[119] filters,[120] channel setting insulating obstacles,[121] and column arrays.[122] Furthermore, iDEP can be employed with both AC and DC fields;[123] DC fields promote overall particle mobility by inducing electrokinetic and DEP transport, whereas AC fields can improve separations that only have an impact on DEP. A few of the most significant discoveries regarding iDEP are categorized according to the kind of dielectrophoretic mode: streaming and trapping iDEP. While the latter offers significant potential for particle enrichment, the former is mostly employed for particle sorting (Fig. 9B). Although iDEP is an effective tool for particle separation and characterization, its use is constrained by the absence of

quantitative characterizations. This constraint can be overcome by Weiss. N. G. and colleagues[127] using a technique that measures the DEP mobility of particles. iDEP is used for protein manipulation; appropriate column arrays are created in microfluidic channels based on the convection diffusion models of positive and negative DEP; and the electric field distribution and protein concentration are computed using numerical simulation. The primary protein aggregates in buffer[128] are captured by DEP. Moreover, brain stem cells and progenitor cells may be distinguished and described using DC-iDEP.[129]

The primary goal of this procedure for contactless DEP (cDEP)[130] is to break the contact between the electrodes and the sample (Fig. 9C), which effectively stops bubbles from forming and lessens device contamination.[126] Using cDEP, a label-free technique for bacterial separation and identification, one can use a non-uniform electric field to separate bacteria and capture them to obtain Raman spectra.[131] H. Shafiee *et al.*[132] distinguished living cells from dead cells using a microfluidic device based on the differences in dielectric between the two types of cells.

A summary of the analysis of several typical dielectrophoretic techniques is given in Table 2.[133–140]

A challenge in the separation of particles using dielectrophoretic forces is that when subjected to these forces, particles in contact with a metal surface tend to adhere to it. This phenomenon is particularly noticeable on some biological cells and potentially useful microelectrodes. Therefore, the particles must be repelled from the high field area to preserve their freedom of movement and to shield them from the potentially harmful high fields and field gradients on the electrode surface. By setting the dielectric polarization rate to be higher than the particle polarization rate,[141] this problem can be resolved. In addition to the above-mentioned approaches, this issue can be resolved using three-dimensional electrode designs. Three-dimensional (3D) electrodes improve the gradient of the electric field and, hence, the capabilities of the system, but they also tend to raise the level of complexity and consequent cost. Bioparticles have been captured, manipulated,[142] accumulated, sorted,[143] focused,[143] and separated using

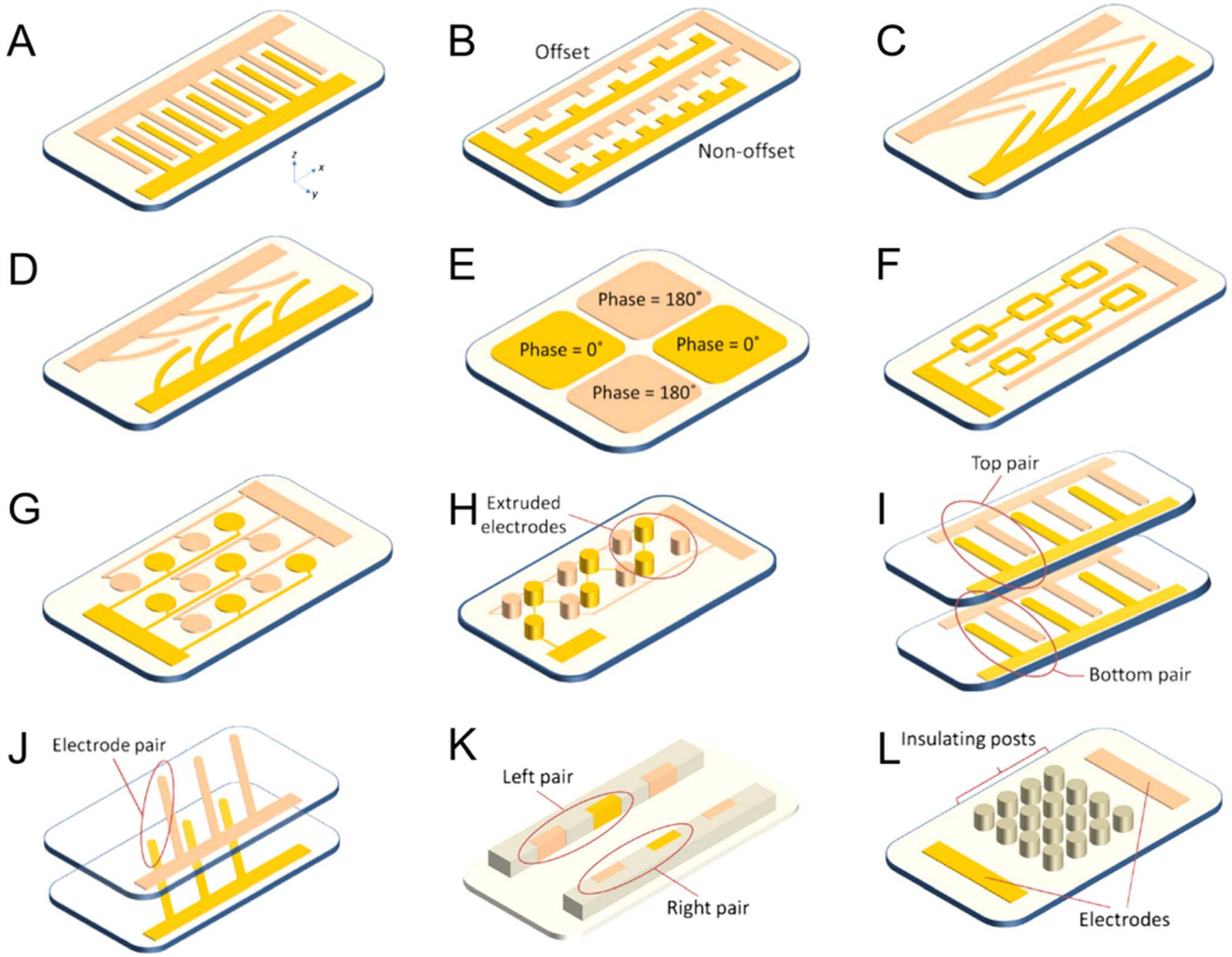

Fig. 8 DEP devices categorized based on the arrangement of microelectrodes:[112] (A) parallel or intersecting, (B) cylindrical, (C) angled, (D) curved, (E) quadrupole, (F) microporous, (G) matrix, (H) extruded, (I and J) top-down pattern, (K) sidewall pattern, and (L) insulator-based or nonpolar.

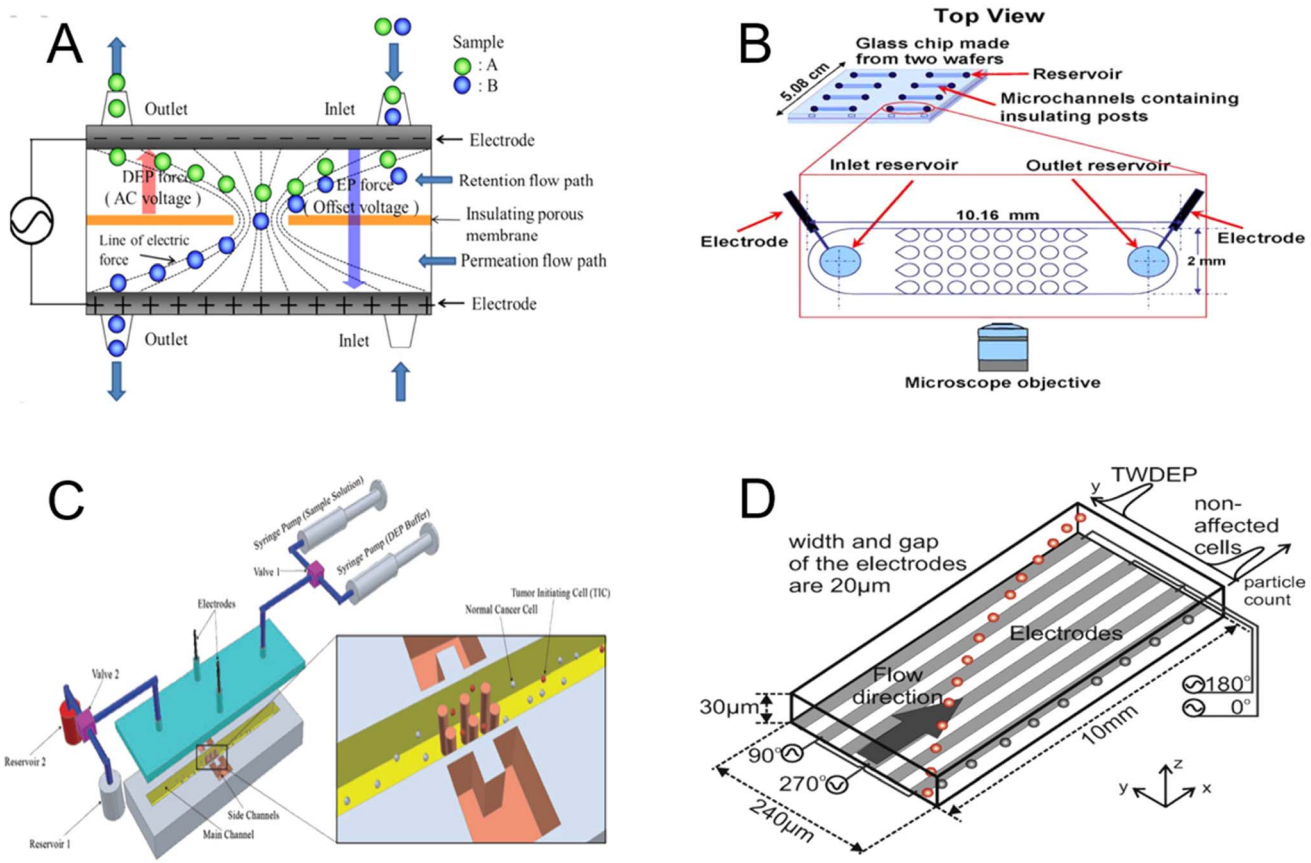

Fig. 9 DEP device classification based on a few principles. (A) Diagram of the separation principle.[124] (B) Chip schematic of proteins controlled by direct current (DC) field and insulator-based dielectric electrophoresis (IDEP).[125] (C) The main channel (yellow) and side channel (pink) in the schematic of the cDEP device are connected by a very thin membrane. An electric field gradient forms in the main channel around the membrane when the conductive side channel is polarized using a linear electrode.[126] (D) Using twDEP for separation.[111]

3D thin-film electrodes. The following examples focus on the design and optimization of 3D electrodes and highlight their applications in DEP systems (Fig. 10). A constant electric field is supplied to the channel height by the 3D electrode on the chip sidewall (Fig. 10A). An even electric field is supplied to the channel height by the 3D electrode on the chip sidewall. One method of processing samples is to catch small particles on the electrode and gather larger particles at the device outlet (Fig. 10A(ii)). Another method is to gather small particles at the device outlet after they are freed from the electrode during the process of rinsing with a buffer solution (Fig. 10A(iii)).[144] For the purpose of dielectrophoretic production, an AC field with alternating on/off control is applied between the interdigitated electrodes. Particles are transported into relative outlets by the twDEP at different velocities or directions by combining 3D electrodes (Fig. 10C).[146] To assist in cell separation, a series of oblique interdigitated electrodes on the microchannel floor are slanted 45° with regard to the direction of flow (Fig. 10D).[147] The posts and orifices on opposing sides of the solidified liquid metal electrodes provide an uneven 3D field across the channel width. Another approach is the uneven 3D field throughout the channel width caused by the orifices and posts located on opposing sides of the liquid metal electrodes that have solidified (Fig. 10E).[148]

3.2 Biological applications

Driving bioparticles is a crucial task, and using a label-free approach like DEP offers benefits for bioparticle manipulation. Consequently, DEP is employed in micro devices for the purposes of separating, focusing, classifying, capturing, concentrating, filtering, and patterning microparticles, cells, and bioparticles. The dielectrophoretic force, the electrical characteristics of the medium, and the particle volume are all connected. DEP has made it feasible to characterize and manipulate biological particles such as neurons, blood cells, β cells in the pancreas, chromosomes, proteins, and viruses. When an AC field is provided at a specific frequency, DEP can be used to separate particles that have distinct sign polarizabilities as they move in various directions.[149] In order to achieve the separation effect, blood cells and other micron-sized entities are separated to the low-field region, while sub-micron and nanoparticles such as DNA, mitochondria, and viruses are separated to the DEP high-field region on the microelectrodes. Particles associated with cancer and other disorders can be quickly separated and detected in biological samples based on size differences, with the particles being distributed to distinct locations.[150] After washing away larger plasma particles to reveal

Table 2 Summary of biological particles manipulation and separation dielectrophoretic techniques

Microfluidic technique	Electrophoretic mechanism	Driving mode	Particle types	Particle size	Resolution	Strengths	Limitations	Ref.
Electrode-based DEP (eDEP)	Direct electric field	Electrode drive	Cells, proteins, biomolecules	1–100 μm	90–99%	Generate high field gradients with low voltage applied	Produce the Joule heating, disintegrate electrodes	133 and 134
CDEP (contactless DEP)	Indirect electric field	Electrode drive	Bacteria, virus, exosomes	20 nm–10 μm	90–99%	The integrity of the electrode structure is excellent, reduce electrolysis	Inadequate durability and repeatability	135 and 136
Curvature induced DEP (c-iDEP)	Indirect electric field	Non-electrode drive	Cells, viruses, proteins	1 nm–10 μm	80–95%	Greater use of chip area and simplicity of fabrication	Less coverage has been presented	137 and 138
Insulator gradient DEP (iGDEP)	Indirect electric field	Non-electrode drive	Bacteria, viruses, DNA	1 nm–10 μm	70–95%	Swift and precise collection from a variety of sources	Analytes and targets must be inserted into the device from a single side	139 and 140

the drug delivery nanoparticles in the DEP chip, the different nanoparticles from plasma are extracted and analysed.[151]

Electrode designs differ based on the specific application requirements. The elliptical channel circumference of the microelectrode edge field, which was produced by the negative dielectrophoretic force toward the centre of the microchannel allowed Yu. C.[152] to design and create a three-dimensional dielectrophoretic particle focusing channel that focused biological cells. Deterministic lateral displacement provides nanoscale resolution for biological sample separation, while DEP offers the benefit of simple tuning. By combining the two, these benefits can be fully utilized.[153] Using a modified polystyrene microsphere containing anti-mouse IgG and a substrate equipped with three-dimensional microelectrodes to control particle flow and collect particles in a cage region, the microfluidic device captures particles under a high electric field (n-DEP) to isolate the necessary analytes and label antibodies.[154] Along with performing parametric modelling and dielectrophoretic force quantification, it can also simulate the distribution of electric fields.[155] The primary goal of forming square and triangle loops is to bend the lines of the electric field inside the microfluidic channel, which forces the cells to frequently visit the capture area and expedites the process of cell concentration and separation.[156] The system performs quick, automatic molecular labelling analysis and includes a fluid device to sort, isolate, and burst target cells from samples. Target particles and cells in the suspension media can be manipulated, differentiated, and separated[157] (Fig. 11).[158–160]

Different designs are employed for DNA capture in the DEP applications on DNA. In microfluidic systems, DEP can effectively separate and capture individual DNA molecules.[161] Dielectrophoretic capture is a viable technique for capturing polarizable molecules within the system. DNA molecules can be fixed in a stretched shape when exposed to a powerful, high-frequency electric field.[162] In a microfluidic chip, the DNA bridge establishes a connection between electrodes and can rapidly capture stretched long DNA fragments. It can also separate double-stranded λ-DNA molecules by direct current electrophoresis and capture them by alternating current dielectrophoresis (Fig. 12A).[163] Due to the fact that dielectrophoretic force is mostly dependent on DNA molecule length, electrodeless DEP can also collect and concentrate single-stranded and double-stranded DNA molecules. Dielectrophoretic force at a particular capture voltage grows with the length of DNA molecules and has a high dispersion.[166] Through careful selection of the electric field and parameters, one can selectively capture a range of DNA molecules and delete another range of DNA molecules. Compared to microelectrodes, insulator-based DEP turns out to be a more cost-effective option for collecting DNA.[167]

Intrinsic mechanical and electrical property indicators are useful cell-specific characteristics for drug screening, customized therapy, and disease diagnostics. Typical mechanical characteristics encompass shear modulus, and steady-state viscosity,[168] among other things. These characteristics are crucial in determining adhesion, migration, polarization, and differentiation, among other cellular and subcellular

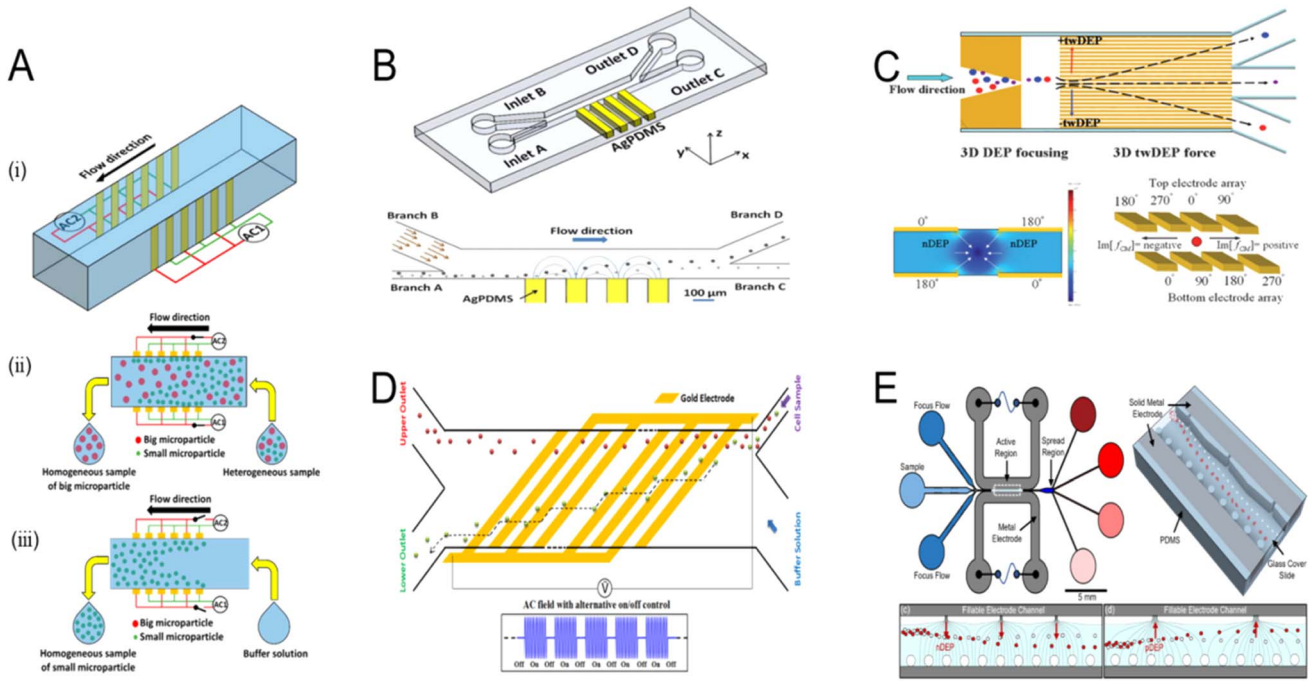

Fig. 10 Dielectrophoresis microfluidic chip design in three dimensions. (A) Electrodes on the side walls to provide a consistent electric field directed towards the channel height. (i) Diagram of the suggested microfluidic device; (ii) diagram of microparticle separation; (iii) diagram of microparticle aggregation.[144] (B) PDMS microdevice with 3D sidewall composite electrodes and a built microdevice separation mechanism.[145] (C) The 3D electrode design diagram.[146] (D) Schematic of the design and principle for the microfluidic cell separation using continuous flow DEP.[147] (E) Diagram of a microfluidic device that uses a focused flow to separate samples from consecutive non-uniformities in the field.[148]

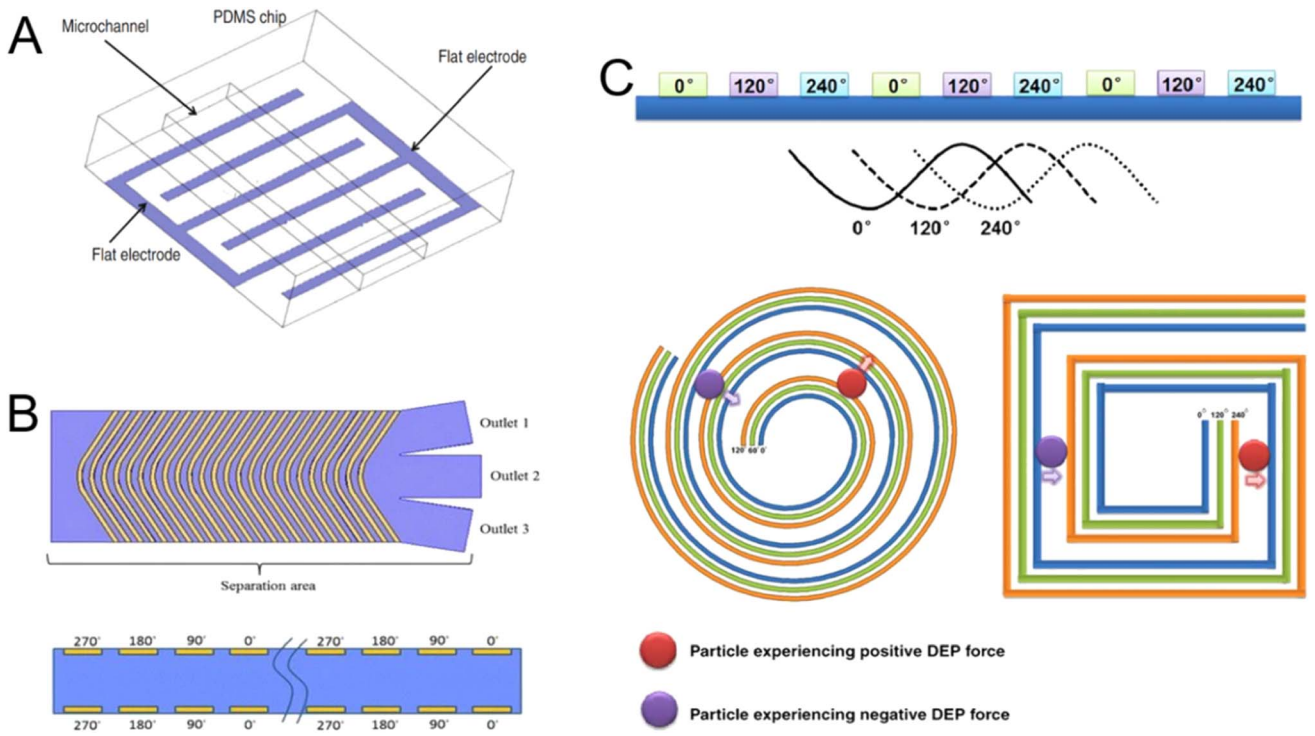

Fig. 11 DEP structural design for biological applications. (A) Schematic of electrodes.[158] (B) A chevron electrode configuration eliminating the erratic electric field and unexpected DEP and twDEP behaviours of the cells.[159] (C) Spiral electrode array intended to create an electric field phase gradient in a three-phase travelling-wave DEP system.[160]

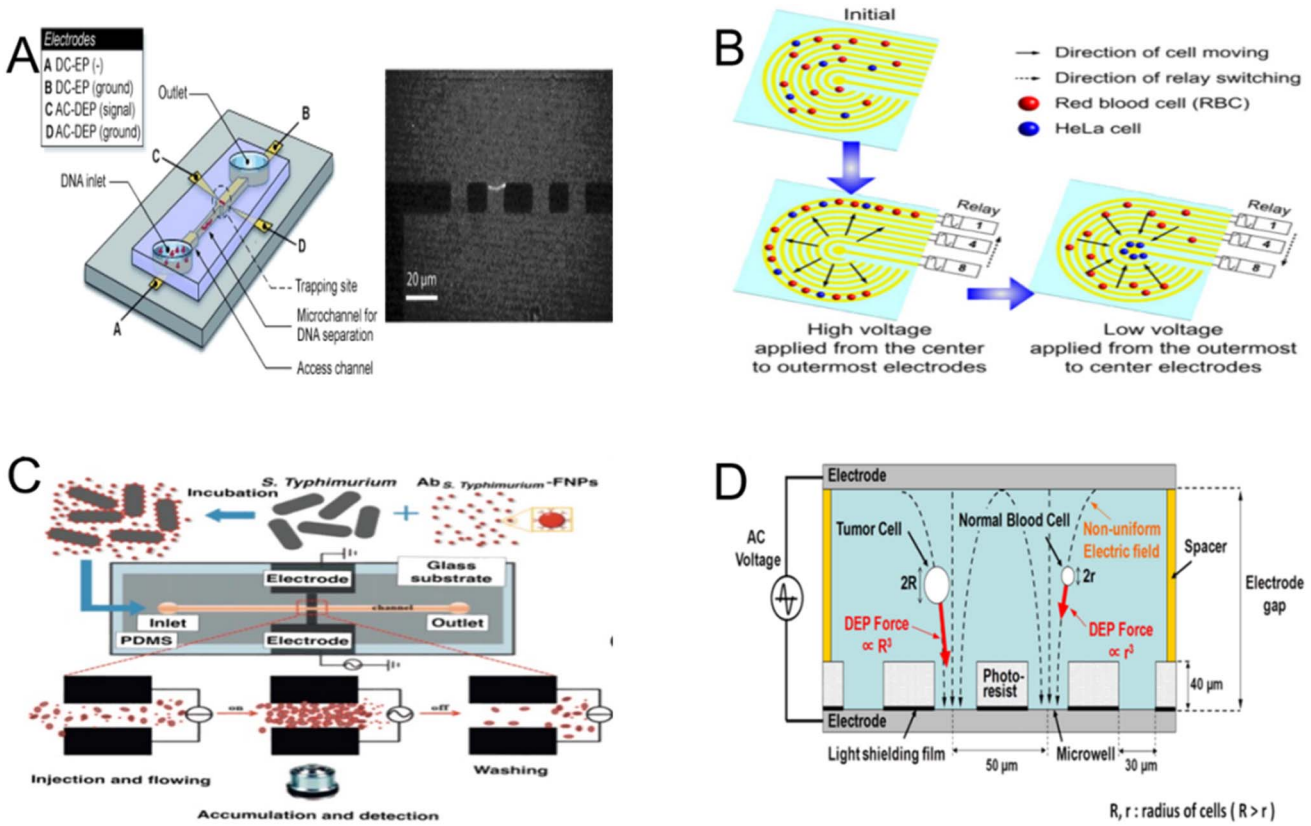

Fig. 12 Illustrations of DEP in biological contexts. (A) In microfluidic chips, alternating current DEP is used to collect double-stranded λ-DNA molecules between aluminum electrodes. (B) Working principle of employing DEP in a ramping electric field to isolate HeLa cells.[163] (C) Bacterial cells trapped and accumulated for detection. When an electric field is generated, *S. typhimurium* is injected into a microfluidic channel and trapped at the detection region by pDEP.[164] (D) CTC enrichment technique principle. A DEP force is applied to the cells, and as a result of the non-uniformity of the electric field is exposed on the bottom surface of each microwell in this design.[165]

processes,[169] and they shed light on the health of cells and disorders involving them. Cell manipulation involves the use of various control strategies. Examples of mechanical techniques are micropipette absorption tests[170] and cell transport analyzers.[171] Electrical properties are widely used in addition to mechanical ones to characterize the growth, viability, and traits of various cell types. Electrical characteristics such as the conductivity and dielectric constant of the membrane and cytoplasm are intimately associated with the morphology and molecular makeup of the cell.[172] A range of techniques such as electrical rotation methods, cell-matrix impedance sensing,[173] and impedance flow cytometry[174] can be used for measurement. Numerous applications in biology and biotechnology from basic cell-based screening to surface immunoassays for diagnostics are based on the manipulation of cells (Fig. 12B).[164]

DEP detects and separates cells using the electrical characteristics of the cells indicated above. While every cell has different dielectric characteristics based on factors such as species, complexity, stage of the cell cycle, and fluctuations in vitality.[175] The skill of cell sorting lays the essential foundation for further medical and diagnostic procedures. This distinct dielectric property can be utilized by AC-DEP to detect and isolate diseased or damaged cells, as well as to identify and separate cells from other particles. One method for identifying circulating tumor cells (CTCS) is to use the physical differences between tumor cells, such as size, charge, density, and expression of biomarkers, to finally lead to target cell separation (Fig. 12D).[165] For example, the herringbone microfluidic system developed by S. L. Stott *et al.*[176] uses antibody-biomarker binding to harvest CTCs from blood. While this technique works well for capturing CTCs in general, it is not able to distinguish between CTCs with identical biomarker expression. DEP is capable of addressing many of the previously mentioned challenges.[177] Its specificity is notably high, as evidenced by the distinct actions displayed by various cell types under a consistent medium conductivity.[178] In DEP spectroscopy, Z. Çağlayan *et al.*[179] proposed a method that uses the inherent dielectric properties of suspended cells to separate CTCs from blood without directly analysing the properties of the cell membrane and cytoplasm, in contrast to conventional methods that rely on theoretical assumptions and complex modelling.

DEP is a valuable cell enrichment method in addition to cell isolation. DEP can enrich small groups of cells from cell mixtures,[180] and identify stem cells and differentiated cell populations.[181] Controlling the size and frequency of the applied field can enable fine control of pumping and manipulation of cell-specific bioparticles by driving the interfacial polarization of cells, colloids, and artificial microelectrode

surfaces, resulting in the formation of bulk flow and particle motion.[182] The frequency is different, and the layout of the cells is also different. For example, when the frequency is lower than the crossover frequency, the cells rearrange into chains and move to the electrode edge.[183] When the frequency is close to the crossover frequency, the cells move individually to the collection area and aggregate along the electrode edge (Fig. 12C).[164] Dielectrophoretic force can be used to arrange cell arrays such as negative dielectrophoretic traps can capture cells at the minimum electric field.[184] With a variety of addressable DEP traps integrated into microchannels a few millimetres long, using nested electrode structures to bulk enrich live yeast cells through DEP, the combination of microfluidic channels and dielectrophoretic electrode structures allowed for the development of more complicated cell processing.

Furthermore, DEP has been utilized in viruses in addition to DNA and cells. DEP has been applied to lyse different viruses as well as to isolate, define, assess, and react to physiological and pathological changes. Due to the tiny size of the virus, surface conductivity plays an essential part. As a result, when the conductivity of the suspended medium increases in the range of 1–10 mS m^{-1}, the cross frequency also increases, which can have an effect on DEP analysis.[185] Improvements are still needed in the application of DEP to viruses. For example, there is a lack of research on DEP at the individual virus level, while other factors such as electrothermal influence or Brownian force have a greater impact on viruses than larger particles.[186] Besides the above-mentioned applications, DEP can be integrated with other technologies to achieve more versatile applications. For example, combined with light induction, optical-induced DEP (ODEP) is another mechanism based on light-induced dielectrophoresis,[182] which has also been proposed for extracting the density and mass[180] as well as electrical[181] and mechanical properties[182] of particles. Similar to DEP, this method also relies on alternating non-uniform electric field to polarize and drive particles. The difference between them is that ODEP can effectively use optical projection images to generate virtual electrodes, which means that this method can dynamically and programmatically manipulate cells without any metal electrodes.

Microfluidic chip can combine the multifunctional fluid processing in the microfluidic device with precise engineering tools in order to further promote the manipulation capability for more systematic analysis and practical biomedical applications.[187] The advantage of DEP lies in the simplicity, reliability, and affordability of the required device for its operation. Additionally, DEP offers electronic control and comprehensive programmability.[188]

4. Advances of fluidic electric control mode

Droplet microfluidic is a new technology for manipulating small volumes of liquid on microfluidic chips, using discontinuous fluid control systems. The droplet microfluidic system uses two immiscible fluids to form droplets *via* shear force and interfacial tension at the microchannel interface. One of the fluids acts as the continuous phase, forming monodisperse droplets. W/O-type droplets and O/W-type droplets are the two general categories into which droplets can be classified based on the distinct water phase or oil phase of the dispersed phase. The W/O-type droplets are classified as the dispersed phase of water and the continuous phase of oil, while O/W-type droplets are the opposite. The initial and crucial phase in conducting droplet manipulation and application research is droplet generation. Massive amounts of sophisticated biological and chemical experiments can be conducted using droplets thanks to precisely planned droplet processes such as droplet fusion, droplet fission, droplet classification, and droplet mixing. Cell carriers can also be employed *via* microspheres created by microfluidic technology.

The two electrical driving techniques discussed herein, namely electroosmotic flow (EOF) and electrowetting-on-dielectric (EWOD), are widely used in droplet creation and propulsion. Chatterjee, D. *et al.*[189] proposed that by applying alternating or direct current potential to the electrode under the dielectric, the droplets in contact with the dielectric surface will move, merge and mix. They demonstrated the feasibility of manipulating droplets, moving liquid by using only appropriate voltage and frequency, which can be empirically predicted based on its frequency-dependent complex dielectric constant.

Electroosmosis depends on the surface charge of the electrode/electrolyte interface. Most materials acquire a fixed surface charge when they contact liquids containing ions. The surface charge attracts counterions from the solution and repels co-ions from the surface to maintain local charge neutrality. Therefore, excess charge accumulates near the electrode surface, forming an electrical double layer (EDL). The interlayer charge will move under the action of the external electric field, at this time the solid is stationary, and the hetero charged ion and its solvation layer on the surface will move directionally to the electrode surface under the electric field. Due to the viscosity of the fluid, the fluid around the ions moves, causing the so-called electroosmosis (Fig. 13A).[190] Electrowetting-on-dielectric (EWOD) is an effective method of droplet manipulation. It uses the electrostatic energy stored in the dielectric layer between the droplet and the electrode to change the local surface tension and droplet contact angle. The difference in contact angle at the droplet edge generates a net capillary force to drive the droplet (Fig. 13B).[191] Another method of propelling the droplets, continuous electrowetting (CEW), which takes use of the change in surface tension between liquid (liquid metal) and liquid (dielectric), powers rotating liquid micro-motors and micro-pumps. According to this theory, the drivable medium must be limited by filling liquid (some electrolyte) containing liquid metal. The system needs two liquids since it is based on surface tension electric control of aqueous liquid droplet movement. Different surface tensions are produced at the two bending liquid surfaces as a result of the applied voltage, which results in a pressure differential that drives movement. The liquid–solid surface tension at the liquid–solid–gas interface is what drives electrowetting (EW) and EWOD (Fig. 13C).[192] The

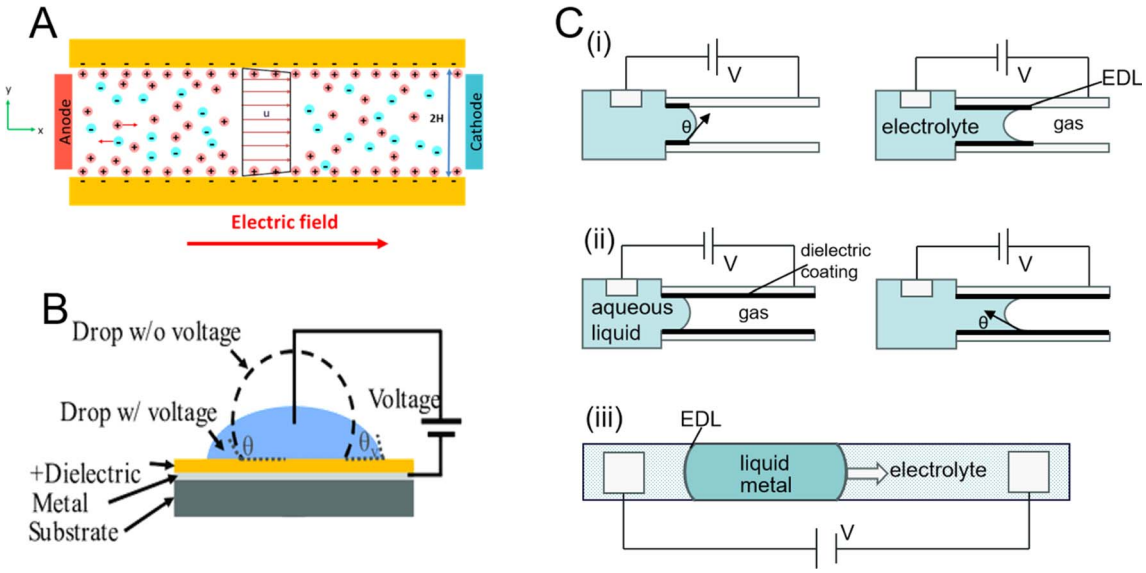

Fig. 13 (A) Diagram showing the typical electroosmosis process in a microchannel. The electric double layer, which is predominant in cations, is subject to a tangential force from the electric field. The fluid travels as a result of this tangential force.[190] (B) Typical external voltage EWOD setup to assess change in contact angle.[191] (C) Driving principle comparison diagrams connected to EWOD: (i) electrowetting (EW). (ii) Electrowetting-on-dielectric (EWOD).[192] (iii) Continuous electrowetting (CEW).

liquid flows into and out of the channel as a result of variations in this tension.

4.1 Electroosmotic flow (EOF)

From chip laboratory equipment for biological applications to fluid flow manipulation of microfluidic chip logic components, the use of microfluidic applications is becoming increasingly prevalent. Electroosmotic flow (EOF)-driven movement and focusing occur simultaneously, making it the most ideal for reduction reactions when compared to the chemistry and fluid dynamics because of its quick speed, compatibility, and affordable instrument requirements. A charged surface or porous solid medium submerged in an electrolyte solution will flow at a set speed when an electric field is provided to both ends of the surface or medium. This phenomenon is known as electroosmotic flow. In microfluidic chip injection methods, electric injection predominates, wherein the sample is propelled into the separation channel through electroosmotic flow induced by an applied electric field (Fig. 14A).[193] The coulombic force that the electric field exerts on the net moving charge in the solution is what causes electroosmotic flow (Fig. 14).[194] Because of the preferential adsorption of certain ions from the solution or the dissociation of surface groups, the solid surface in the solution frequently carries a charge. Excess counterions that are equal in number to the surface charge but opposite in sign must exist in the liquid next to the charged surface for there to be electrical neutrality. This is another electroosmotic flow principle (Fig. 14C).[195] An electrical double layer is formed by the charged surface and counterions. To determine the role of the ion polarization layer, A. Alizadeh *et al.*[197] discussed the physicochemical phenomena caused by the double-layer interaction when the characteristic length of the conductive medium decreases from micrometre to nanometre. The relative size of the EDL and the intermediate domain channel relative to the EDL thickness are both factors affecting the transport phenomenon. Depending on the nature of the applied electric field and device configuration, electroosmosis can be classified as DC electroosmosis, time-periodic electroosmosis, AC electroosmosis[198] and induced charge electroosmosis.

Practical applications of EOF encompass the following. EOF can be used to regulate fluid dynamic diffusion to achieve continuous cell separation, and combining the stability of pressure-driven flow and the adjustability of EOF, it can be easily adjusted to suit different particle size ratios of separation. The separation mechanism of particles depends on the frequency and voltage of the applied electric field. Under high-frequency conditions, particles are positioned in a way consistent with DEP, under low-frequency conditions, positioning is a strong coupling between gravity, the vertical component of dielectric force and the Stokes resistance induced by alternating current electroosmotic flow on the particles (Fig. 14D).[196] This low-frequency state of fluid flow is a useful tool for capturing particles on the electrode surface using coplanar electrodes.[199] The coupling of alternating current electroosmosis and DEP can achieve cell separation that cannot be achieved based on DEP alone.[200] J. Wu *et al.*[201] used alternating current electroosmotic flow to bring bacteria to the capture area or stagnation area, to achieve faster detection with impedance spectroscopy.

The drive and control of electroosmotic flow, though advantageous, have some limitations. One of the disadvantages of EOF is that its initial phase and sample injection are unstable. For instance, several dynamic processes occur during the first stage of EOF, such as the establishment of a temperature gradient in the electrolyte and matrix, the propagation of

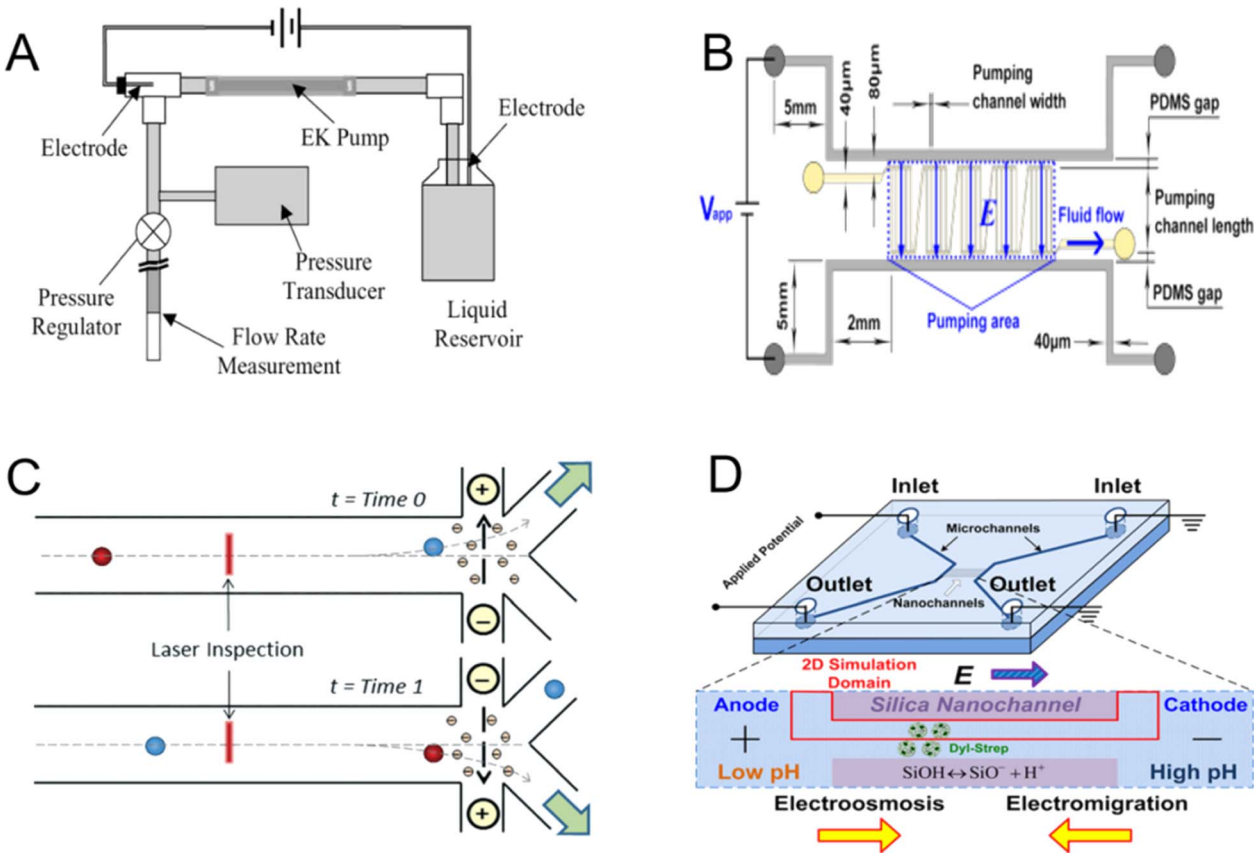

Fig. 14 (A) Schematic of the setup for EOF micropump characterization. The volume flow rate in a tube is measured by pumping liquid with the EOF pump.[193] (B) Schematic of the five-stage EOF pump.[194] (C) Sorting of electroosmotic cells using direct current (DC). Solvated negative ions in the counterionic layer along the positively charged microchannel floor migrate to the oppositely charged electrode after laser inspection and cell identification. This causes the surrounding liquid to be drawn for cell transport to various outlets.[195] (D) Proteins concentrated toward the anode (low pH) end when the electromigration effect is stronger and near the cathode (high pH) end when the electroosmotic effect is more prominent.[196]

the electric field, and the capacitive charging of the double layer. In order to address this issue, G. Tang *et al.*[202] developed a mathematical model that is three dimensional and described how Joule heat affects the electroosmotic flow transport of limited samples in microfluidic channels. They came to the conclusion *via* a numerical simulation that Joule heat speeds up sample transport and modifies the sample band shape, making it lower in peak and wider. S. V. Puttaswamy *et al.*[203] combined negative DEP (nDEP) focusing and alternating current electroosmotic flow (AC EOF) technique to perform electric-driven cell sorting, overcoming Faraday reaction, to achieve three different functions of focusing, transporting cells to detection site and reloading unsorted cells. The production of electroosmotic flow, for instance, requires a high voltage power source, which has issues with power consumption, safety, and space, making it difficult to miniaturize the system. Research studies focus on enhancing several facets of EOF technology, such as refining low-cost fabrication methods, ensuring reliable device performance, and enabling efficient droplet manipulation at lower voltages. Similarly, the EOF technology can be further optimized to allow parallel manipulations of even larger arrays of liquid droplets, thereby massively boosting its functionality in biological sensing applications.

4.2 Electrowetting-on-dielectric (EWOD)

Adding a dielectric layer to the metal surface can apply a high voltage, called electrowetting-on-dielectric (EWOD). Unlike traditional electrowetting[204] and continuous electrowetting,[205] EWOD has been proven to not only switch droplets between beading and wetting but also move droplets along the desired path on the surface. Polarizable and conductive droplets are initially stationary on the hydrophobic surface when a potential is applied between the droplet and the insulating counter electrode below the droplet. The droplet of conductive liquid initially forms a contact angle with the solid hydrophobic insulator (solid outline). Applying a voltage between the droplet and the counter electrode below the insulator reduces the solid–liquid interfacial energy, resulting in a decrease in the angle and an improvement of the wetting of the droplet on the solid[206] (Fig. 15A).[206] The improvement of wetting is due to the reduction of the effective solid–liquid interfacial energy by the electrostatic energy stored in the capacitor formed by the droplet-insulator-electrode system. Using solid insulators as

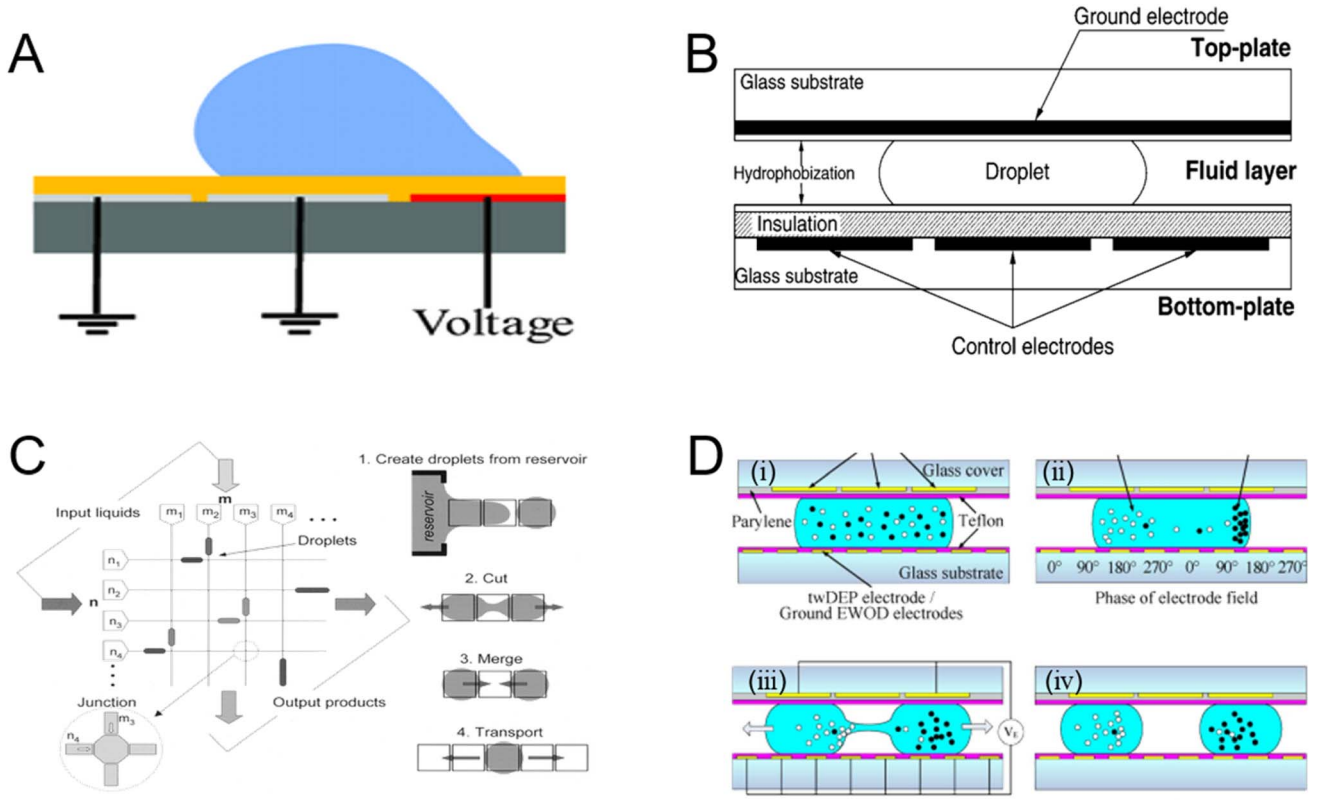

Fig. 15 (A) Open coplanar EWOD design.[206] (B) Diagram illustrating the cross-section of the electrowetting chip. The interfacial tension imbalance that results from applying an electric field to only one side of a droplet leads to the bulk flow of the droplet.[207] (C) Envisioned digital microfluidic circuit that can be utilized as a lab-on-a-chip or micro total analysis device, together with the four essential droplet activities required: liquid droplets are created, transported, sliced, and merged using electrowetting techniques.[208] (D) Procedures for separating particles within droplets using twDEP and EWOD.[209]

dielectrics, larger surface energies can be obtained at lower electric fields, and the surface chemistry can be better controlled. It is possible to switch droplets between beading and wetting and also to move droplets along the desired path on the surface (Fig. 15B).[207] Multiple droplets can be physically moved by electrical signals, without any physical pumps or valves, to achieve simple microfluidic devices.[208]

EWOD has been proven to provide complete droplet functionality from droplet injection, delivery, merging, and mixing to splitting (Fig. 15C).[208] Numerous microfluidic processes including droplet transport, mixing, splitting, and distribution are made possible by chips based on EWOD. Two sets of opposite planar electrodes are fabricated on glass, directly controlling the surface tension, under certain conditions; the repeatable transmission of droplets has been proven and this speed is nearly 100 times higher than the electric method of transmitting droplets on the solid surface.[210] Mixing can be done by making two droplets directly contact and allowing them to merge.[208] Zhao *et al.*[209] suggested that there are now two types of in-droplet separation and concentration. Particle transport by twDEP and droplet splitting by EWOD are the primary microfluidic operations (Fig. 15D). Two parallel plates are sandwiched by a droplet containing mixed particles (Fig. 15D(i)). Particles of type B (black) are transported and concentrated on the right side under the twDEP produced by the bottom electrodes, whereas particles of type A (white) are transported on the left side (Fig. 15D(ii)). The droplet divides into two daughter droplets under EWOD. With the twDEP electrodes on the bottom plate grounded, the two electrodes on the top plate are triggered (Fig. 15D(iii)). Consequently, type A particles are concentrated in the left droplet while type B particles are concentrated in the right daughter droplet (Fig. 15D(iv)). To fully describe and predict the flow, other influences must also be considered, including the viscous resistance of the solvent, the flow resistance of the channel, and the induced pressure caused by the difference in electroosmotic mobility of different parts of the complex channels.

Applications for EWOD in cell detection and microbiology are varied. Applications for clinical chemistry involve the detection of analytes, including metabolites, electrolytes, and liver function indicators. Researchers V. Srinivasan *et al.*[211] showed that the electrowetting process of droplets does not result in the loss of enzyme activity, and that it can measure glucose in physiological fluids while also transferring human whole blood, plasma, urine, and saliva droplets in a dependable and repeatable way. Barbulovic-Nad, I. *et al.*[212] compared the vitality and growth of electrowetting-driven and non-driven

cells, and found no significant difference, suggesting that the effect of droplet driving on cell vitality, proliferation and protein expression can be neglected. Single-cell analysis plays a crucial role in comprehending cellular specificity. One category of single-cell assays is label-free, allowing the measurement of cell phenotypes or the isolation of cells based on these phenotypes without altering them using markers such as dyes or antibodies.[213] Microdroplets offer a well-defined and potentially sterile environment for the controlled loading of individual cells, contributing to the miniaturization of cell-based assays.[214] H. Hufnagel *et al.*[215] have described an integrated cell culture lab-on-a-chip for cultivating mammalian cells and delivering them into microfluidic droplets. In a similar vein, Yu, Z. *et al.*[216] devised an intelligent droplet microfluidic system capable of selectively cracking and real-time sorting of single cells. The system utilizes droplet microinjection and image recognition technology for selective cracking and real-time sorting of individual cells, automating the collection of cracked single-cell droplet samples. It exhibits notable advantages in precision, throughput, automation, and pollution-free operation. For nucleic acid analysis process, first it needs to extract and purify DNA or RNA from crude samples. S. Paul *et al.*[217] adopt droplet-to-droplet (DTD) form of liquid–liquid extraction (LLE) method for microfluidic DNA separation. Electrowetting microfluidic can easily handle two-phase liquid systems, and ionic liquids encapsulate DNA molecules by electrostatic interactions and extract nucleic acids from impurities. The sample droplets and extractant droplets are separated by a simple mixing. In addition to extraction, sometimes nucleic acids also need to be pre-concentrated, especially for real samples, because the sample volume is reduced, the detection limit of microfluidic devices may be affected.[218] S. Kalsi *et al.*[219] pre-concentrated bacterial DNA in 1 mL urine sample to 2 μL droplet, thereby detecting the antibiotic resistance gene of *Klebsiella pneumoniae* in the sample.

Electrowetting on dielectric (EWOD) has distinctive advantages. EWOD can be used to handle micro-scale aqueous liquids, without any second liquid medium. This driving method has many advantages, by electrically changing the wetting of each electrode pattern on the surface, the liquids on these electrodes can be shaped and driven along the active electrodes, simplifying the fabrication and operation of microfluidics.[192] Controlling the surface tension for liquid handling and driving has many advantages in micro-scale applications, and as the liquid handling system becomes smaller, surface tension has a dominant and effective role. Thermal drive devices that leverage surface tension, including thermal capillary,[220] micro-pumping of liquid,[221] and micro-optical switches,[222] are subject to several limitations. These limitations encompass high power consumption, the necessity for liquid heating, rapid evaporation, and a slower operational speed. In contrast to thermal drives, EWOD-based micro drives eliminate the need for liquid heating, offering enhanced speed and reduced power consumption. Furthermore, the EWOD drive technology extends the scope of influence on droplet propulsion, encompassing factors such as gravity, equipment configuration, material properties, temperature, tilt behaviours, compensation methods, energy consumption, response time, physical limitations, and the operation of the autofocus function.[223]

5. Advances of microfluidic-based electrorotation (ROT) mode

Biological particles exhibit rotational motion, and the rotation rate of a particle is influenced by the applied voltage and frequency, as well as the distance of the particle from the centre of the electrode. This unique feature offers an additional method of manipulating particles, providing a subtle control mechanism that can be investigated and used in combination with other electrodynamic methods for increased adaptability in microscale applications.[224]

A typical ROT chip is made up of four metal-based electrodes that are positioned in a mutually orthogonal layout, creating a crisscross, using conventional micro-lithography techniques. With a phase difference of $\pi/2$, each of the four electrodes is coupled to an AC bias potential. A rotating, non-uniform electric field is produced by this arrangement, which torques the suspended cells and causes ROT. ROT does not happen if there is no phase difference voltage between the quadrupole electrodes.[225] In his optimization research, Hughes[226] claims that compared to cone, ellipse, and polynomial electrode structures, the polynomial electrode structure assures uniform torque distribution by finding a workable equilibrium between maximal rotational torque and maximum area. Four sinusoidal signals applied in phase orthogonality to a three-dimensional micromachined polynomial electrode cause rotating torque on the cell.

Within the context of electrical rotation, a rotating electric field has two purposes: first, it creates a dipole moment in the particle; second, it imparts torque to the dipole moment. The coordinated movement causes the particle to rotate, showcasing the flexibility of electric fields in finely adjusting objects at the microscopic level.[227] The electric field is often composed of two oscillating components with phase shifts: one oscillates perpendicular to the direction of the static field, while the other oscillates in the direction of the electrostatic field. Together, these oscillating components produce a rotating electric field that impacts each particle. Electrical rotation is a useful metric when assessing membrane integrity, characterizing cells, and assessing the vitality of cells. The efficient application of Micro-Electro-Mechanical Systems (MEMS) and Micro Total Analysis Systems requires a variety of control functions, such as fluid mixing and non-contact object manipulation in microchannels. Coupled electrical rotation (CER) offers an easy way to use a consistent external RF electric field to control the rotation of dielectric objects.[228]

5.1 Biological applications

Electrorotation emerges as a label-free analytical technique capable of discerning the dielectric properties of cells and effectively distinguishing between various cell lines.[229] While this technique exhibits relatively low parallelism, the dielectric

properties of cells play a pivotal role in characterizing distinct stages and types of cells. Electric field-induced particle rotation serves as a robust technique for assessing the dielectric properties of cell membranes. This method offers the advantage of non-invasive, *in vitro* study of individual cells. Beyond dielectric property measurements, cell rotation can be employed to investigate cell morphology. Its utility extends to applications such as monitoring cell culture[230] and differentiated cell lines.[231] Employing electrorotation provides valuable insights into cellular behaviour and composition, offering a versatile tool for diverse cellular analyses.

The majority of biological investigations involving cells are carried out in batch trials with an emphasis on cell population analysis. For many biological studies, average data are frequently sufficient. Yet, although having the same outward appearance, individual cells differ in terms of important metabolite quantities and particular gene expression. These intrinsic variances between individual cells can occasionally lead to false information in cell-based assay findings from population analysis. Consequently, the examination of individual cells is required for the early detection of mutations within a population of cells.[232] Single-cell manipulation is important for many fields such as biology and medicine, and includes basic movements such as rotation and displacement. As many methods as there are for physically moving, arranging, ensnaring, and joining biological cells, very few studies deal with the regulation of single-cell rotation. While conventional cell analysis provides average population results and some new tools allow single-cell function understanding, they often face limitations in terms of throughput or analysis accuracy. Electrical rotation, although slower in processing, possesses unique capabilities for single-cell characterization. In biological applications such as nuclear transfer,[233] dielectric parameter assessment,[234] cell imaging,[235] and injection,[236] achieving rotation is crucial yet difficult.

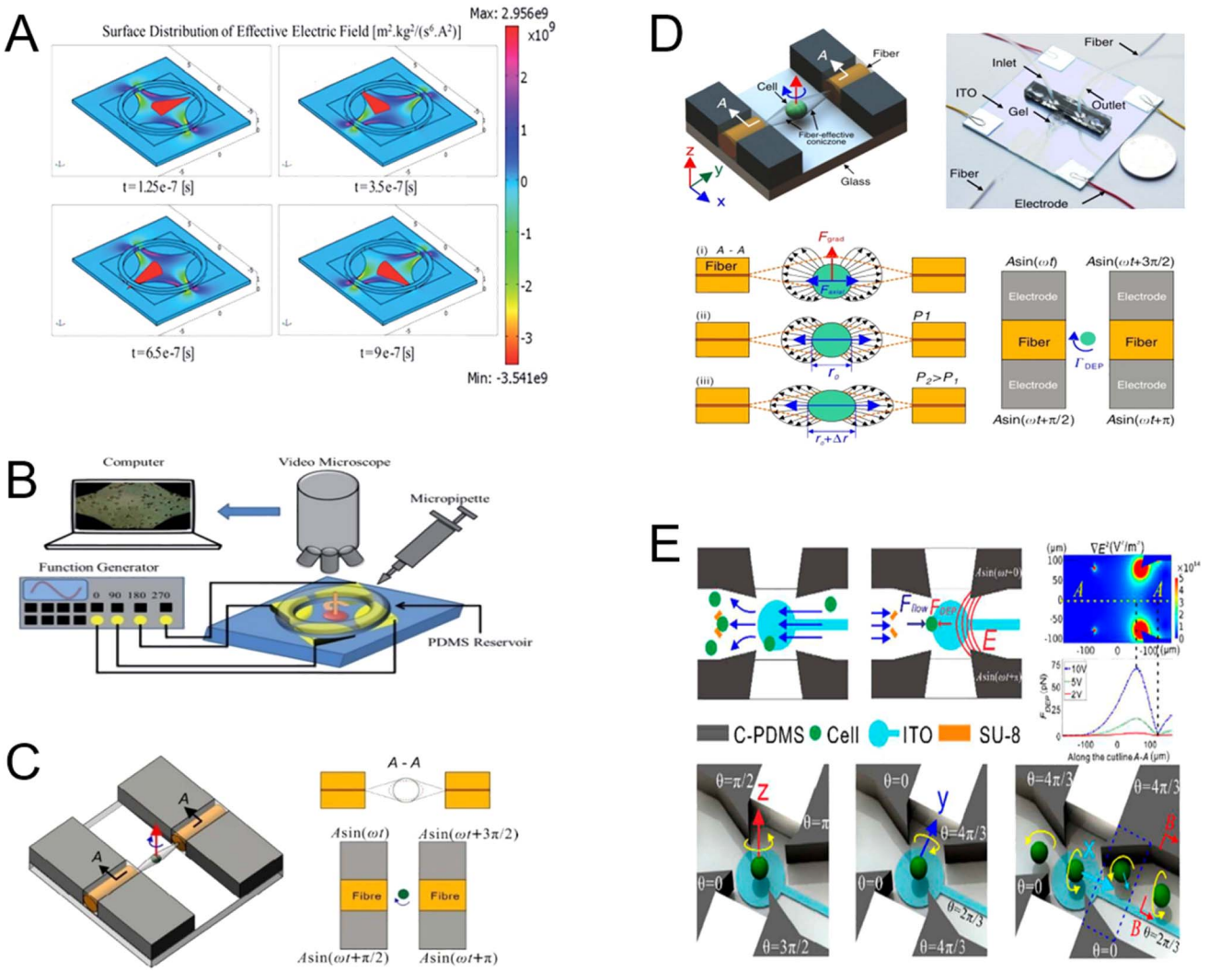

Fig. 16 (A) Effective electric field distribution on the device surface simulated by COMSOL.[239] (B) Using microtubules, a 3 mL cell solution was added to the PDMS reservoir in the ER test setup.[239] (C) Working principle of the microfluidic chip. Optical and electrical stretch devices rotate and stretch cells in particular directions.[240] (D) Principles of electrospinning and the light-trapping and light-stretching process.[241] (E) Operating principle of an ROT chip with 3D cells.[242]

Electrorotation can be synergized with DEP to ascertain the dielectric properties of a single cell. The rotation method induces cell rotation, complemented by negative DEP forces to ensure cells remain unaffected by flow.[237] The underlying principle involves polarizing the cell under an alternating current field. This involves initially applying a dielectrophoretic force to secure the single cell at the centre of a four-set electrode structure, followed by the application of rotational torque to induce electrical rotation of the cell. The differentiation of various cell samples is achieved based on rotational speed.[238] The rotating effective electric field's direction at each instant is depicted in the three-dimensional graphic (Fig. 16A). This method offers high controllability, allowing adjustment of electrical signal parameters to govern rotation speed and direction. For instance, Trainito, C. *et al.*[243] combined negative dielectric power for sphere trapping with electric rotation torque for measuring dielectric properties. Analysing the rotation velocity curve with electric field frequency enabled the estimation of dielectric parameters, proposing different models for determining these properties. After a negative DEP force was applied from the two electrodes, a single cell that had been hydrodynamically trapped by a unit was released by backflow and continued to remain in the spinning chamber (Fig. 16C). According to Vaillier, C. *et al.*,[244] human cells rotated by a fluid vortex created by the interaction of DEP forces and Joule heat in the absence of a revolving electric field. To tackle unstable cell rotation, numerical simulations were conducted to analyse electric fields under different signal configurations, cell self-adaptation effects, and single-cell suspension. To create rotational torque on the cell, a sinusoidal signal with an orthogonal phase stimulates the polynomial electrode (Fig. 16B). In experiments, spatial positioning and 3D rotation were achieved through electrode signal configuration, facilitating full-angle imaging of cells and subsequent contour reconstruction using appropriate algorithms.[245] The corresponding AC signals were produced by the *Z*, *Y*, and *X* axes of cell rotation (Fig. 16E).[242] In this process, dielectric electrophoresis captures individual cells, allowing the estimation of their dielectric properties such as cytoplasm and membrane permittivity through the application of rotating electric fields.[246] Conventional DEP technology typically requires at least three electrodes to generate a rotating electric field for inducing cell rotation. L. Huang *et al.*[247] proposed an innovative microfluidic chip, utilizing polarized cells as additional electrodes for phase shift signals. This approach allows the rotation of single cells using only two planar electrodes, simplifying microdevice structures. S.-I. Han *et al.*[229] conducted measurements of cell dielectric properties by combining a negative dielectrophoretic force with electric rotational torque. The obtained dielectric properties enable the discrimination of target cells from heterogeneous cell mixtures, facilitating the identification of rare cells in peripheral blood amid normal blood cells.

Electrorotation can be applied more effectively with three-dimensional electrodes by means of dielectrophoretic forces. Combining 3D electrodes with microfluidics establishes a closed fluid system, enabling precise single-cell treatment with controlled injection volumes.[248] Electrical rotation can be achieved using either planar electrodes or 3D electrodes, both of which are easy to manufacture. However, the electric field intensity generated by planar electrodes is non-uniform and decays faster in the vertical direction. Since cell rotation speed is influenced by the electric field intensity, this parameter varies significantly at different spatial locations of the electric field generated by planar electrodes.[249] In contrast, the 3D electrode configuration produces a more uniform electric field distribution in the vertical direction, resulting in a consistent and stable cell rotation speed.[250] According to DEP theory, an in-plane rotating electric field is formed in a virtual rotating chamber surrounded by electrodes by applying an AC signal with a 90° phase shift to four vertical electrodes. Cells in this rotating chamber exhibit in-plane rotation corresponding to the rotating electric field. The rate of cell rotation is dependent on the cell type, solution composition, and the electrical parameters of the external electrical signal. A microfluidic chip, equipped with two relative optical fibres and four three-dimensional electrodes, is designed for the simultaneous measurement of multiple physical parameters. This chip is capable of capturing and stretching single cells using optical fibres, as well as rotating single cells using the 3D electrodes. These four electrodes serve as microchannel walls, creating two orthogonal microchannels. The microchannel along the *X*-axis serves as the primary channel for the flow of cell samples. The vertical channel along the *Y*-axis functions as the fibre loading channel, housing two *Y*-axis-aligned single-mode fibres for cell capture and stretching.[241] Addressing challenges in single-cell 3D rotating operation platforms, L. Huang *et al.*[251] devised a top capture section, leveraging the principle of minimum flow resistance to automatically place individual cells in the rotation chamber, enhancing stability. In addition to traditional metal-based microelectrodes, photocoupled microfluidics using digital programming and light activation can achieve cell translation and spin behavior.[252] Electrorotation confines the separated biological particles to a specific electrode structure, so once the biological particles have been separated, electrical rotation is best used as an identification/performance evaluation technique rather than as a separation technique.

6. Design of electrically driven microfluidic chips

6.1 Design of the structure

A microfluidic system is a fluid device that has channels that range in diameter from a few hundred microns to approximately 100 nanometres. Tiny channels result in unexpected features that open up a wide range of unconventional applications. For instance, multiplexing, automation, and high-throughput screening can be accomplished by systems built to handle such small amounts of fluids. The minuscule size of the channels causes special behaviors in fluids that are contrary to assumptions. The causes of this discrepancy include surface tension, fluidic resistance, and energy loss. It takes specific theories and technology to address these unique behaviors. Leading the way in addressing these issues is the scientific

discipline of microfluidics, which provides researchers with practical methods for using and modifying fluids in tiny spaces.[253]

The primary construction of the microfluidic chip consists of two substrate layers (PMMA, PDMS, glass, *etc.*) with sample inlets, detection windows, microchannels, and microstructures. Complementary peripheral equipment includes peristaltic and micro-injection pumps, temperature control systems, and UV, fluorescence, electrochemical, and chromatographic detection components. The integrated electrical equipment, which manages temperature, automates control, takes and analyses pictures, and drives and controls microfluidic flow, is an integral component of the microfluidic chip. Compact electrically driven mechanisms and minimal power consumption are required for microfluidic chips. Numerous researchers have created various micropumps such as the micro-mechanical pump,[254] electrowetting,[255] and electroosmosis,[256] to address these issues. Pei Wen Yen *et al.*[257] constructed a microfluidic pump device for circuit integration to address low power consumption and easy integration with low-voltage drive systems. Munyan[258] and associates have led the way in creating novel electrically driven micropumps that are smoothly incorporated into microfluidic systems. These devices use only tiny voltages (about 10 V) and take advantage of the accumulation of electrolysis gasses to enable pressure-driven pumping. This approach could provide simple, affordable, and readily integrated microfluidic analytical components. Even though there has been a lot of progress in creating microvalves that are appropriate for biological applications, these devices are still costly, large, and energy-intensive due to the off-chip components that are frequently needed for their actuation. For instance, air pressure sources and solenoid valves are required for the actuation of pneumatic polydimethylsiloxane (PDMS) valves, which are commonly found in integrated microfluidic systems.[259] This restriction prevents such valves from being widely used in disposable, inexpensive, and portable microfluidic devices.[260]

In each method employed for inducing fluid motion, the surface characteristics of the device can be harnessed to offer supplementary control. For example, the channel and network of channels can be patterned or modified in terms of their geometrical, chemical, and mechanical characteristics. The sample injection region, the electrophoresis separation channel, and the method for detecting the migrating analytes are the three fundamental components of the design of the microfabricated electrophoresis system. A separation column must be built for electrophoresis applications that are long enough to give the appropriate sensitivity and resolution while taking up just a little bit of space. The migration rate (migration velocity) and diffusion coefficient (*i.e.*, the band broadening rate during electrophoretic migration) must be specified and the separation channel must be folded into a compact geometry. Another crucial step in the separation process is putting the sample into the channel. When non-concentrated and non-focused samples are injected, the region may diffuse and the associated signals of the components may fall below the detectable range, necessitating a longer separation distance to separate the components. Each component can be found within a commensurately short separation distance by injecting concentrated and targeted sample zones. Surface forces are fundamental to electrokinetic pumping and particle manipulation, and they become much more important in micro-dimensions because of the elevated surface-to-volume ratio. Increasing the contact area and contact time of the sample streams is one method of improving the performance of electrokinetic microfluidic mixers. Other methods include constructing irregular flow fields in the mixing channel or implementing various possible schemes, the majority of which entail vertical cross-channel geometry. To increase the contact area in these kinds of devices, a number of microchannel layouts have been proposed, including T-shaped, cross-shaped, double-cross-shaped, and multi-T-shaped arrangements.[261] Where the voltage is switched after the analytes are electrically carried through the separation channel. Volumetric flow, diffusion-based, pressure-driven,[262] nanocapillary array interconnect,[263] and fluid dynamics are examples of common channel geometries.

6.2 Material selection and processing

Innovative materials for the production of microfluidic chips are constantly being developed in tandem with the continual development of micro total analysis systems. Inorganic, organic, hybrid, and composite materials can all be used to describe these materials. Quartz, silicon, and glass are a few examples of inorganic materials used to create a microfluidic chip.[264] An essential component of the semiconductor industry, silicon dioxide was largely used in the early stages of microchip creation. Because of its great purity, large inertia, and effective heat dissipation, crystalline silicon is essential to the manufacturing of microchips. Conventional techniques entail photolithography using standard techniques, followed by wet etching to form microchannels on silicon wafers.[265] Glass microchips are widely used in chemical analysis because of their remarkable optical characteristics. Moreover, a negative charge is present on the glass surface, which promotes consistent electroosmotic flow. The polymers are gas permeable and have surfaces that are suitable for cell culture, in contrast to glass, silicon, and other inorganic materials.[266]

Microfluidic systems possessing a wide range of unique properties have been fabricated by means of the constant development of new materials and creative ways to combine and arrange already existing parts. X. Hou[267] presents a thorough analysis of the benefits and drawbacks of every kind of material, highlighting significant instances of how each has evolved in the creation of microfluidic devices and emphasizing more recent applications. The covalent alteration of PMMA channels to introduce an amine functionality has been reported by Henry *et al.*[268] When compared to unmodified channels, it is discovered that the electroosmotic flow in aminated PMMA microchannels is inverted. It is possible to derivatize the amine group further to create several stable surface chemistries on PMMA channels. Barker *et al.*[269] at NIST treated microchannels by polyelectrolyte multilayer deposition, a non-specific coating

technique. As long as the plastic material has a sizable surface charge to promote electrostatic interactions between the polyelectrolyte and the surface, this coating technique is adaptable and stable for a range of plastic materials. The principal gains offered by this technique are enhanced protein adsorption, increased mass transport efficiency of immune reactants, and consequent reduction in the equilibration time of the immunochemical reactions.[270] Specific application requirements frequently serve as guidance for the selection and processing of materials for microfluidic chips, taking stability, performance, and cost into account. Future developments in this subject could result in the synthesis of new materials and the design of fabrication methods.

7. Conclusion and prospects

This review provides an overview of various electric driving modes and their applications in microfluidic chips. Based on solid particles, electrophoretic techniques drive charged particles, while dielectrophoretic techniques manipulate uncharged particles, and both of them move in a plane. Electrical rotation is primarily utilized for the three-dimensional movement of cells. Depending on the distinct separation media, various electrophoresis techniques such as Capillary electrophoresis, gel electrophoresis, and FFE are appropriate for different biological particles. AC-DEP, DC-DEP, and twDEP are introduced according to the types and gradients of the electric field. Based on droplet driving, EOF and EWOD are applicable to different scenarios. Moreover, it exhibited the distinctive design principle of electric-driven microfluidic chips and future development trends. Future advances will encompass developing high-throughput systems for the detection of many biomarkers, broadening applications across multiple fields[271–273] and creating portable equipment ideal for urgent field inspection, such as rapid point-of-care testing.[274–276] Additionally, artificial intelligence integrated with microfluidic chips improve the precise control of droplet motion and dynamic assessment of biomolecular interactions. In summary, microfluidic-based particle manipulation techniques have broad application prospects in disease diagnosis and biomedical engineering.

Data availability

This is a review paper. No primary research results, software or code have been included and no new data were generated or analysed as part of this review. This review cited some data from published papers, and matched data can be obtained from the matched published papers.

Conflicts of interest

The authors declare no competing interests.

Acknowledgements

This work was supported from Key research and development project of Ministry of Science and Technology of China (No. 2017YFA0205300), Projects of International Cooperation and Exchanges of the National Natural Science Foundation of China (No. 82020108017), the National Natural Science Foundation of China (No. 62227815, 81921002), Shanghai Science and Technology Commission standard project (No. 21DZ2203200).

References

1 J. Jiang, X. Cui, Y. Huang, D. Yan, B. Wang, Z. Yang, M. Chen, J. Wang, Y. Zhang and G. Liu, Advances and Prospects in Integrated Nano-oncology, *Nano Biomed. Eng.*, 2024, **16**(2), 152–187.
2 Q. Tian, Y. Mu, Y. Xu, Q. Song, B. Yu, C. Ma, W. Jin and Q. Jin, An integrated microfluidic system for bovine DNA purification and digital PCR detection, *Anal. Biochem.*, 2015, **491**, 55–57.
3 M. Chen, S. Lin, C. Zhou, D. Cui, H. Haick and N. Tang, From conventional to microfluidic: progress in extracellular vesicle separation and individual characterization, *Adv. Healthcare Mater.*, 2023, **12**(8), 2202437.
4 S. Yatsushiro, Y. Yamaguchi, S. Yamamura, Y. Shinohara, Y. Baba and M. Kataoka, Highly sensitive DNA detection with a combination of 2 DNA-intercalating dyes for microchip electrophoresis, *J. Pharm. Biomed. Anal.*, 2011, **55**(1), 202–205.
5 J.-J. Qian, H.-Y. Ji, H. Cong, H.-M. Wang and Q.-H. Jin, Application of Polydimethylsiloxane/Glass Microchips for Fast Electrophoretic Separation of Serum High-density Lipoprotein Subclasses, *Chin. J. Anal. Chem.*, 2012, **40**(2), 230–235.
6 S. Zhao, Y. Huang, F. Ye, M. Shi and Y.-M. Liu, Determination of intracellular sulphydryl compounds by microchip electrophoresis with selective chemiluminescence detection, *J. Chromatogr. A*, 2010, **1217**(36), 5732–5736.
7 S. Lin, X. Zhi, D. Chen, F. Xia, Y. Shen, J. Niu, S. Huang, J. Song, J. Miao and D. Cui, A flyover style microfluidic chip for highly purified magnetic cell separation, *Biosens. Bioelectron.*, 2019, **129**, 175–181.
8 V. Jokinen, P. Sakha, P. Suvanto, C. Rivera, S. Franssila, S. E. Lauri and H. J. Huttunen, A microfluidic chip for axonal isolation and electrophysiological measurements, *J. Neurosci. Methods*, 2013, **212**(2), 276–282.
9 Q. Sun, S. Li, R. Lin, G. Zhao, J. Lu, B. Liu, M. Hu, W. Wang, X. Yang and Y. Wei, hUC-MSCs therapy for Crohn's disease: efficacy in TNBS-induced colitis in rats and pilot clinical study, *Ebiomedicine*, 2024, **103**, 105128.
10 Z. Yu, S. Lin, F. Xia, Y. Liu, D. Zhang, F. Wang, Y. Wang, Q. Li, J. Niu and C. Cao, ExoSD chips for high-purity immunomagnetic separation and high-sensitivity detection of gastric cancer cell-derived exosomes, *Biosens. Bioelectron.*, 2021, **194**, 113594.
11 X. Zhi, L. Chen, S. Gao, S. Lin, D. Chen, J. Niu, Z. Jin, B. Ji, L. Kang, X. Ding, W. Xin, J. Wang, D. Cui and H. Yang, Temperature gap drives directed diffusion in microfluidic chip system, *Microfluid. Nanofluid.*, 2019, **23**(3), 40.

12 H. Tang, J. Niu, X. Pan, H. Jin, S. Lin and D. Cui, Topology optimization based deterministic lateral displacement array design for cell separation, *J. Chromatogr. A*, 2022, **1679**, 463384.
13 C.-C. Hong, P.-H. Chang, C.-C. Lin and C.-L. Hong, A disposable microfluidic biochip with on-chip molecularly imprinted biosensors for optical detection of anesthetic propofol, *Biosens. Bioelectron.*, 2010, **25**(9), 2058–2064.
14 X. Ding, P. Li, S.-C. S. Lin, Z. S. Stratton, N. Nama, F. Guo, D. Slotcavage, X. Mao, J. Shi, F. Costanzo and T. J. Huang, Surface acoustic wave microfluidics, *Lab Chip*, 2013, **13**(18), 3626–3649.
15 Y. Zhang, A. Zhou, S. Chen, G. Z. Lum and X. Zhang, A perspective on magnetic microfluidics: Towards an intelligent future, *Biomicrofluidics*, 2022, **16**(1), 011301.
16 M. R. Hossan, D. Dutta, N. Islam and P. Dutta, Electric field driven pumping in microfluidic device, *Electrophoresis*, 2018, **39**(5–6), 702–731.
17 T. B. Jones, Basic theory of dielectrophoresis and electrorotation, *IEEE Eng. Med. Biol. Mag.*, 2003, **22**(6), 33–42.
18 P. Tathireddy, Y.-H. Choi and M. Skliar, Particle AC electrokinetics in planar interdigitated microelectrode geometry, *J. Electrost.*, 2008, **66**(11), 609–619.
19 M. Dawod and D. S. Chung, High-sensitivity capillary and microchip electrophoresis using electrokinetic supercharging, *J. Separ. Sci.*, 2011, **34**(20), 2790–2799.
20 J. V. Pagaduan, V. Sahore and A. T. Woolley, Applications of microfluidics and microchip electrophoresis for potential clinical biomarker analysis, *Anal. Bioanal. Chem.*, 2015, **407**, 6911–6922.
21 A. C. De Peña, D. Zimmer, E. Gutterman-Johns, N. M. Chen, A. Tripathi and C. M. Bailey-Hytholt, Electrophoretic Microfluidic Characterization of mRNA-and pDNA-Loaded Lipid Nanoparticles, *ACS Appl. Mater. Interfaces*, 2024, **16**(21), 26984–26997.
22 D. Wu, J. Qin and B. Lin, Electrophoretic separations on microfluidic chips, *J. Chromatogr. A*, 2008, **1184**(1–2), 542–559.
23 S. Hoffstetter-Kuhn, R. Kuhn and H. Wagner, Free flow electrophoresis for the purification of proteins: I. Zone electrophoresis and isotachophoresis, *Electrophoresis*, 1990, **11**(4), 304–309.
24 K. J. M. Bishop, A. M. Drews, C. A. Cartier, S. Pandey and Y. Dou, Contact Charge Electrophoresis: Fundamentals and Microfluidic Applications, *Langmuir*, 2018, **34**(22), 6315–6327.
25 V. M. Ugaz and J. L. Christensen, Electrophoresis in microfluidic systems, *Microfluidic Technologies for Miniaturized Analysis Systems*, 2007, pp. 393–438.
26 V. A. Galievsky, A. S. Stasheuski and S. N. Krylov, Capillary Electrophoresis for Quantitative Studies of Biomolecular Interactions, *Anal. Chem.*, 2015, **87**(1), 157–171.
27 C. Heller, Principles of DNA separation with capillary electrophoresis, *Electrophoresis*, 2001, **22**(4), 629–643.
28 B. L. Karger and A. Guttman, DNA sequencing by CE, *Electrophoresis*, 2009, **30**(S1), S196–S202.
29 J. E. Melanson, N. E. Baryla and C. A. Lucy, Dynamic capillary coatings for electroosmotic flow control in capillary electrophoresis, *Trac. Trends Anal. Chem.*, 2001, **20**(6–7), 365–374.
30 J. M. Cunliffe, N. E. Baryla and C. A. Lucy, Phospholipid bilayer coatings for the separation of proteins in capillary electrophoresis, *Anal. Chem.*, 2002, **74**(4), 776–783.
31 Q. Tu, J.-C. Wang, Y. Zhang, R. Liu, W. Liu, L. Ren, S. Shen, J. Xu, L. Zhao and J. Wang, Surface modification of poly(dimethylsiloxane) and its applications in microfluidics-based biological analysis, *Rev. Anal. Chem.*, 2012, **31**(3–4), 177–192.
32 S. M. Adem, E. Mansfield, J. P. Keogh, H. K. Hall Jr and C. A. Aspinwall, Practical considerations for preparing polymerized phospholipid bilayer capillary coatings for protein separations, *Anal. Chim. Acta*, 2013, **772**, 93–98.
33 Y. Liang, D. Tao, J. Ma, L. Sun, Z. Liang, L. Zhang and Y. Zhang, Hydrophilic monolith based immobilized enzyme reactors in capillary and on microchip for high-throughput proteomic analysis, *J. Chromatogr. A*, 2011, **1218**(20), 2898–2905.
34 R. Wu, Z. Wang, W. Zhao, W. S.-B. Yeung and Y. S. Fung, Multi-dimension microchip-capillary electrophoresis device for determination of functional proteins in infant milk formula, *J. Chromatogr. A*, 2013, **1304**, 220–226.
35 Y. T. Kim, J. Y. Choi, Y. Chen and T. S. Seo, Integrated slidable and valveless polymerase chain reaction–capillary electrophoresis microdevice for pathogen detection, *RSC Adv.*, 2013, **3**(22), 8461–8467.
36 S. Jeeawoody, K. A. Yamauchi, A. Su and A. E. Herr, Laterally aggregated polyacrylamide gels for immunoprobed isoelectric focusing, *Anal. Chem.*, 2020, **92**(4), 3180–3188.
37 S. Haeberle and R. Zengerle, Microfluidic platforms for lab-on-a-chip applications, *Lab Chip*, 2007, **7**(9), 1094–1110.
38 Y. Liu, C. Li, Z. Li, S. D. Chan, D. Eto, W. Wu, J. P. Zhang, R.-L. Chien, H. G. Wada, M. Greenstein and S. Satomura, On-chip quantitative PCR using integrated real-time detection by capillary electrophoresis, *Electrophoresis*, 2016, **37**(3), 545–552.
39 K. D. Dorfman, S. B. King, D. W. Olson, J. D. Thomas and D. R. Tree, Beyond gel electrophoresis: Microfluidic separations, fluorescence burst analysis, and DNA stretching, *Chem. Rev.*, 2013, **113**(4), 2584–2667.
40 N. Khan, J. Cheng, J. P. Pezacki and M. V. Berezovski, Quantitative Analysis of MicroRNA in Blood Serum with Protein-Facilitated Affinity Capillary Electrophoresis, *Anal. Chem.*, 2011, **83**(16), 6196–6201.
41 C.-C. Hsieh, A. Balducci and P. S. Doyle, Ionic Effects on the Equilibrium Dynamics of DNA Confined in Nanoslits, *Nano Lett.*, 2008, **8**(6), 1683–1688.
42 J. Vlassakis and A. E. Herr, Joule heating-induced dispersion in open microfluidic electrophoretic cytometry, *Anal. Chem.*, 2017, **89**(23), 12787–12796.
43 J. Kim, J. P. Hilton, K.-A. Yang, R. Pei, M. Stojanovic and Q. Lin, Nucleic acid isolation and enrichment on a microchip, *Sens. Actuators, A*, 2013, **195**, 183–190.

44 C. Heller, Separation of double-stranded and single-stranded DNA in polymer solutions: I. Mobility and separation mechanism, *Electrophoresis*, 1999, **20**(10), 1962–1976.
45 J. Hui, J. M. Majikes and K. R. Riley, Analysis of DNA Origami Nanostructures Using Capillary Electrophoresis, *Anal. Chem.*, 2023, **95**(51), 18783–18792.
46 B. D. Aguda, Y. Kim, M. G. Piper-Hunter, A. Friedman and C. B. Marsh, MicroRNA regulation of a cancer network: Consequences of the feedback loops involving miR-17-92, E2F, and Myc, *Proc. Natl. Acad. Sci. U. S. A.*, 2008, **105**(50), 19678–19683.
47 X. Li, D. Li, W. Zhou, Y. Chai, R. Yuan and Y. Xiang, A microRNA-activated molecular machine for non-enzymatic target recycling amplification detection of microRNA from cancer cells, *Chem. Commun.*, 2015, **51**(55), 11084–11087.
48 D. W. Wegman, L. T. Cherney, G. M. Yousef and S. N. Krylov, Universal Drag Tag for Direct Quantitative Analysis of Multiple MicroRNAs, *Anal. Chem.*, 2013, **85**(13), 6518–6523.
49 E. Ban, D.-K. Chae and E. J. Song, Simultaneous detection of multiple microRNAs for expression profiles of microRNAs in lung cancer cell lines by capillary electrophoresis with dual laser-induced fluorescence, *J. Chromatogr. A*, 2013, **1315**, 195–199.
50 P. Zhang, J. Zhang, C. Wang, C. Liu, H. Wang and Z. Li, Highly Sensitive and Specific Multiplexed MicroRNA Quantification Using Size-Coded Ligation Chain Reaction, *Anal. Chem.*, 2014, **86**(2), 1076–1082.
51 J.-L. Viovy, Electrophoresis of DNA and other polyelectrolytes: Physical mechanisms, *Rev. Mod. Phys.*, 2000, **72**(3), 813–872.
52 P. Y. Lee, J. Costumbrado, C.-Y. Hsu and Y. H. Kim, Agarose gel electrophoresis for the separation of DNA fragments, *J. Vis. Exp.*, 2012, (62), e3923.
53 J. Wang, A. D. Gonzalez and V. M. Ugaz, Tailoring Bulk Transport in Hydrogels through Control of Polydispersity in the Nanoscale Pore Size Distribution, *Adv. Mater.*, 2008, **20**(23), 4482–4489.
54 M. Hügle, O. Behrmann, M. Raum, F. T. Hufert, G. A. Urban and G. Dame, A lab-on-a-chip for free-flow electrophoretic preconcentration of viruses and gel electrophoretic DNA extraction, *Analyst*, 2020, **145**(7), 2554–2561.
55 P. Agrawal and K. D. Dorfman, Microfluidic long DNA sample preparation from cells, *Lab Chip*, 2019, **19**(2), 281–290.
56 A. E. Gomez Martinez and A. E. Herr, Programmed cell-death mechanism analysis using same-cell, multimode DNA and proteoform electrophoresis, *ACS Meas. Sci. Au*, 2021, **1**(3), 139–146.
57 J. B. Burton, C. L. Ward, D. M. Klemet and T. H. Linz, Incorporation of thermal gels for facile microfluidic transient isotachophoresis, *Anal. Methods*, 2019, **11**(37), 4733–4740.
58 T. Konishi, T. Kusumoto, Y. Hiroyama, A. Kobayashi, T. Mamiya and S. Kodaira, Induction of DNA strand breaks and oxidative base damages in plasmid DNA by ultra-high dose rate proton irradiation, *Int. J. Radiat. Biol.*, 2023, **99**(9), 1405–1412.
59 V. M. M. Haberland, S. Magin, G. Iliakis and A. Hartwig, Impact of Manganese and Chromate on Specific DNA Double-Strand Break Repair Pathways, *Int. J. Mol. Sci.*, 2023, **24**(12), 10392.
60 M. Viefhues, J. Regtmeier and D. Anselmetti, Fast and continuous-flow separation of DNA-complexes and topological DNA variants in microfluidic chip format, *Analyst*, 2013, **138**(1), 186–196.
61 M. Kircher and J. Kelso, High-throughput DNA sequencing-concepts and limitations, *Bioessays*, 2010, **32**(6), 524–536.
62 D. Kohlheyer, G. A. J. Besselink, S. Schlautmann and R. B. M. Schasfoort, Free-flow zone electrophoresis and isoelectric focusing using a microfabricated glass device with ion permeable membranes, *Lab Chip*, 2006, **6**(3), 374–380.
63 P. Couceiro and J. Alonso-Chamarro, Fluorescence Imaging Characterization of the Separation Process in a Monolithic Microfluidic Free-Flow Electrophoresis Device Fabricated Using Low-Temperature Co-Fired Ceramics, *Micromachines*, 2022, **13**(7), 1023.
64 A. Manz and J. C. T. Eijkel, Miniaturization and chip technology. What can we expect?, *Pure Appl. Chem.*, 2001, **73**(10), 1555–1561.
65 R. Wildgruber, G. Weber, P. Wise, D. Grimm and J. Bauer, Free-flow electrophoresis in proteome sample preparation, *Proteomics*, 2014, **14**(4–5), 629–636.
66 K. Y. C. Fung, C. Cursaro, T. Lewanowitsch, L. Cosgrove and P. Hoffmann, A Combined Free-Flow Electrophoresis and DIGE Approach to Compare Proteins in Complex Biological Samples, in *Electrophoretic Separation of Proteins: Methods and Protocols*, ed. B. T. Kurien and R. H. Scofield, Springer, New York, 2019, pp 403–415.
67 A. Zhang, J. Xu, X. Li, Z. Lin, Y. Song, X. Li, Z. Wang and Y. Cheng, High-Throughput Continuous-Flow Separation in a Micro Free-Flow Electrophoresis Glass Chip Based on Laser Microfabrication, *Sensors*, 2022, **22**(3), 1124.
68 S. Jezierski, L. Gitlin, S. Nagl and D. Belder, Multistep liquid-phase lithography for fast prototyping of microfluidic free-flow-electrophoresis chips, *Anal. Bioanal. Chem.*, 2011, **401**(8), 2651–2656.
69 P. Novo and D. Janasek, Current advances and challenges in microfluidic free-flow electrophoresis—A critical review, *Anal. Chim. Acta*, 2017, **991**, 9–29.
70 A. Han, K. Hosokawa and M. Maeda, Activity measurement of protein kinase and protein phosphatase by microchip phosphate-affinity electrophoresis, *Anal. Biochem.*, 2012, **421**(2), 782–784.
71 M. Wang, G. T. Roman, M. L. Perry and R. T. Kennedy, Microfluidic Chip for High Efficiency Electrophoretic Analysis of Segmented Flow from a Microdialysis Probe and *in Vivo* Chemical Monitoring, *Anal. Chem.*, 2009, **81**(21), 9072–9078.
72 L. Sun, G. Zhu, X. Yan, Z. Zhang, R. Wojcik, M. M. Champion and N. J. Dovichi, Capillary zone

electrophoresis for bottom-up analysis of complex proteomes, *Proteomics*, 2016, **16**(2), 188–196.
73 M. Piotrowska, K. Ciura, M. Zalewska, M. Dawid, B. Correia, P. Sawicka, B. Lewczuk, J. Kasprzyk, L. Sola, W. Piekoszewski, B. Wielgomas, K. Waleron and S. Dziomba, Capillary zone electrophoresis of bacterial extracellular vesicles: A proof of concept, *J. Chromatogr. A*, 2020, **1621**, 461047.
74 Z. Zhu, J. J. Lu and S. Liu, Protein separation by capillary gel electrophoresis: A review, *Anal. Chim. Acta*, 2012, **709**, 21–31.
75 R. Bhimwal, R. R. Rustandi, A. Payne and M. Dawod, Recent advances in capillary gel electrophoresis for the analysis of proteins, *J. Chromatogr. A*, 2022, **1682**, 463453.
76 F. Duša, A. Kubesová, J. Šalplachta and D. Moravcová, Capillary isoelectric focusing – The role of markers of isoelectric point and recent applications in the field, *Trac. Trends Anal. Chem.*, 2023, **162**, 117018.
77 J. Dai, J. Lamp, Q. Xia and Y. Zhang, Capillary Isoelectric Focusing-Mass Spectrometry Method for the Separation and Online Characterization of Intact Monoclonal Antibody Charge Variants, *Anal. Chem.*, 2018, **90**(3), 2246–2254.
78 Z. Malá and P. Gebauer, Recent progress in analytical capillary isotachophoresis (2018 - March 2022), *J. Chromatogr. A*, 2022, **1677**, 463337.
79 Z. Malá, P. Gebauer and P. Boček, Recent progress in analytical capillary isotachophoresis, *Electrophoresis*, 2015, **36**(1), 2–14.
80 V. Datinská, I. Voráčová, J. Berka and F. Foret, Preparative concentration of nucleic acids fragments by capillary isotachophoretic analyzer, *J. Chromatogr. A*, 2018, **1548**, 100–103.
81 S. Terabe, Capillary Separation: Micellar Electrokinetic Chromatography, *Annu. Rev. Anal. Chem.*, 2009, **2**, 99–120.
82 G. Hancu, B. Simon, A. Rusu, E. Mircia and A. Gyéresi, Principles of micellar electrokinetic capillary chromatography applied in pharmaceutical analysis, *Adv. Pharm. Bull.*, 2013, **3**(1), 1–8.
83 C. Fanali, Enantiomers separation by capillary electrochromatography, *Trac. Trends Anal. Chem.*, 2019, **120**, 115640.
84 Y. Xue, X. Gu, Y. Wang and C. Yan, Recent advances on capillary columns, detectors, and two-dimensional separations in capillary electrochromatography, *Electrophoresis*, 2015, **36**(1), 124–134.
85 P.-E. Bodet, I. Salard, C. Przybylski, F. Gonnet, C. Gomila, J. Ausseil and R. Daniel, Efficient recovery of glycosaminoglycan oligosaccharides from polyacrylamide gel electrophoresis combined with mass spectrometry analysis, *Anal. Bioanal. Chem.*, 2017, **409**, 1257–1269.
86 S. Magdeldin, S. Enany, Y. Yoshida, B. Xu and Y. Zhang, Basics and recent advances of two dimensional-polyacrylamide gel electrophoresis, *Clin. Proteomics*, 2014, **11**, 1–10.
87 C. Li and T. Arakawa, Agarose native gel electrophoresis of proteins, *Int. J. Biol. Macromol.*, 2019, **140**, 668–671.
88 A. Miglio, M. T. Antognoni, C. Maresca, C. Moncada, F. Riondato, E. Scoccia and V. Mangili, Serum protein concentration and protein fractions in clinically healthy Lacaune and Sarda sheep using agarose gel electrophoresis, *Vet. Clin. Pathol.*, 2015, **44**(4), 564–569.
89 C.-G. Guo, Z. Shang, J. Yan, S. Li, G.-Q. Li, R.-Z. Liu, Y. Qing, L.-Y. Fan, H. Xiao and C.-X. Cao, A tunable isoelectric focusing *via* moving reaction boundary for two-dimensional gel electrophoresis and proteomics, *Talanta*, 2015, **137**, 197–203.
90 A. S. Zarabadi, J. Pawliszyn and M. Hajialamdari, Development of a multichannel microfluidic system with Schlieren imaging microscopy for online chip-based moving boundary electrophoresis, *J. Chromatogr. A*, 2017, **1484**, 93–97.
91 S. T. Krauss, D. Ross and T. P. Forbes, Separation and detection of trace fentanyl from complex mixtures using gradient elution moving boundary electrophoresis, *Anal. Chem.*, 2019, **91**(20), 13014–13021.
92 J. Voldman, Electrical forces for microscale cell manipulation, *Annu. Rev. Biomed. Eng.*, 2006, **8**, 425–454.
93 S. Hu, Y. Wang, Y. Wang, X. Chen and R. Tong, Dielectrophoretic separation and purification: from colloid and biological particles to droplets, *J. Chromatogr. A*, 2024, 465155.
94 B. Çetin and D. Li, Dielectrophoresis in microfluidics technology, *Electrophoresis*, 2011, **32**(18), 2410–2427.
95 A. R. Minerick, R. Zhou, P. Takhistov and H. C. Chang, Manipulation and characterization of red blood cells with alternating current fields in microdevices, *Electrophoresis*, 2003, **24**(21), 3703–3717.
96 A. Jaffe and J. Voldman, Multi-frequency dielectrophoretic characterization of single cells, *Microsyst. Nanoeng.*, 2018, **4**(1), 23.
97 Y. Kang, D. Li, S. A. Kalams and J. E. Eid, DC-Dielectrophoretic separation of biological cells by size, *Biomed. Microdevices*, 2008, **10**, 243–249.
98 C. J. Lentz, S. Hidalgo-Caballero and B. H. Lapizco-Encinas, Low frequency cyclical potentials for fine tuning insulator-based dielectrophoretic separations, *Biomicrofluidics*, 2019, **13**(4), 44114.
99 P. Gascoyne, C. Mahidol, M. Ruchirawat, J. Satayavivad, P. Watcharasit and F. F. Becker, Microsample preparation by dielectrophoresis: isolation of malaria, *Lab Chip*, 2002, **2**(2), 70–75.
100 X. Liang, K. Graham, A. Johannessen, D. Costea and F. Labeed, Human oral cancer cells with increasing tumorigenic abilities exhibit higher effective membrane capacitance, *Integr. Biol.*, 2014, **6**(5), 545–554.
101 J. Yang, Y. Huang, X.-B. Wang, F. F. Becker and P. R. Gascoyne, Differential analysis of human leukocytes by dielectrophoretic field-flow-fractionation, *Biophys. J.*, 2000, **78**(5), 2680–2689.
102 T. Z. Jubery, S. K. Srivastava and P. Dutta, Dielectrophoretic separation of bioparticles in microdevices: A review, *Electrophoresis*, 2014, **35**(5), 691–713.

103 R. Pethig, Dielectrophoresis: Status of the theory, technology, and applications, *Biomicrofluidics*, 2010, **4**(2), 022811.
104 H.-W. Su, J. L. Prieto and J. Voldman, Rapid dielectrophoretic characterization of single cells using the dielectrophoretic spring, *Lab Chip*, 2013, **13**(20), 4109–4117.
105 J. Niu, S. Lin, Y. Xu, S. Tong, Z. Wang, S. Cui, Y. Liu, D. Chen and D. Cui, A stepwise multi-stage continuous dielectrophoresis separation microfluidic chip with microfilter structures, *Talanta*, 2024, **279**, 126585.
106 M. Koklu, S. Park, S. D. Pillai and A. Beskok, Negative dielectrophoretic capture of bacterial spores in food matrices, *Biomicrofluidics*, 2010, **4**(3), 034107.
107 C. J. Ramirez-Murillo, J. M. de los Santos-Ramirez and V. H. Perez-Gonzalez, Toward low-voltage dielectrophoresis-based microfluidic systems: A review, *Electrophoresis*, 2021, **42**(5), 565–587.
108 S. K. Srivastava, J. L. Baylon-Cardiel, B. H. Lapizco-Encinas and A. R. Minerick, A continuous DC-insulator dielectrophoretic sorter of microparticles, *J. Chromatogr. A*, 2011, **1218**(13), 1780–1789.
109 B. G. Hawkins and B. J. Kirby, Electrothermal flow effects in insulating (electrodeless) dielectrophoresis systems, *Electrophoresis*, 2010, **31**(22), 3622–3633.
110 I. F. Cheng, C.-C. Chung and H.-C. Chang, High-throughput electrokinetic bioparticle focusing based on a travelling-wave dielectrophoretic field, *Microfluid. Nanofluid.*, 2011, **10**(3), 649–660.
111 S. van den Driesche, V. Rao, D. Puchberger-Enengl, W. Witarski and M. J. Vellekoop, Continuous cell from cell separation by traveling wave dielectrophoresis, *Sens. Actuators, B*, 2012, **170**, 207–214.
112 M. R. Buyong, J. Yunas, A. A. Hamzah, B. Yeop Majlis, F. Larki and N. Abd Aziz, Design, fabrication and characterization of dielectrophoretic microelectrode array for particle capture, *Microelectron. Int.*, 2015, **32**(2), 96–102.
113 H. Chai, J. Zhu, Y. Feng, F. Liang, Q. Wu, Z. Ju, L. Huang and W. Wang, Capillarity Enabled Large-Array Liquid Metal Electrodes for Compact and High-Throughput Dielectrophoretic Microfluidics, *Adv. Mater.*, 2024, **36**(21), 2310212.
114 K. P. Chen, J. R. Pacheco, M. A. Hayes and S. J. Staton, Insulator-based dielectrophoretic separation of small particles in a sawtooth channel, *Electrophoresis*, 2009, **30**(9), 1441–1448.
115 J. Zhu, T.-R. J. Tzeng, G. Hu and X. Xuan, DC dielectrophoretic focusing of particles in a serpentine microchannel, *Microfluid. Nanofluid.*, 2009, **7**, 751–756.
116 B. H. Lapizco-Encinas, B. A. Simmons, E. B. Cummings and Y. Fintschenko, Insulator-based dielectrophoresis for the selective concentration and separation of live bacteria in water, *Electrophoresis*, 2004, **25**(10-11), 1695–1704.
117 C.-P. Jen and T.-W. Chen, Trapping of cells by insulator-based dielectrophoresis using open-top microstructures, *Microsyst. Technol.*, 2009, **15**, 1141–1148.
118 P. K. Thwar, J. J. Linderman and M. A. Burns, Electrodeless direct current dielectrophoresis using reconfigurable field-shaping oil barriers, *Electrophoresis*, 2007, **28**(24), 4572–4581.
119 Y. K. Cho, S. Kim, K. Lee, C. Park, J. G. Lee and C. Ko, Bacteria concentration using a membrane type insulator-based dielectrophoresis in a plastic chip, *Electrophoresis*, 2009, **30**(18), 3153–3159.
120 C. Iliescu, G. Xu, F. C. Loe, P. L. Ong and F. E. Tay, A 3-D dielectrophoretic filter chip, *Electrophoresis*, 2007, **28**(7), 1107–1114.
121 Y. Kang, B. Cetin, Z. Wu and D. Li, Continuous particle separation with localized AC-dielectrophoresis using embedded electrodes and an insulating hurdle, *Electrochim. Acta*, 2009, **54**(6), 1715–1720.
122 E. B. Cummings and A. K. Singh, Dielectrophoresis in microchips containing arrays of insulating posts: theoretical and experimental results, *Anal. Chem.*, 2003, **75**(18), 4724–4731.
123 C. V. Crowther and M. A. Hayes, Refinement of insulator-based dielectrophoresis, *Analyst*, 2017, **142**(9), 1608–1618.
124 M. Hakoda, Development of dielectrophoresis separator with an insulating porous membrane using DC-Offset AC Electric Fields, *Biotechnol. Prog.*, 2016, **32**(5), 1292–1300.
125 B. H. Lapizco-Encinas, S. Ozuna-Chacón and M. Rito-Palomares, Protein manipulation with insulator-based dielectrophoresis and direct current electric fields, *J. Chromatogr. A*, 2008, **1206**(1), 45–51.
126 R. Martinez-Duarte, Microfabrication technologies in dielectrophoresis applications—A review, *Electrophoresis*, 2012, **33**(21), 3110–3132.
127 N. G. Weiss, P. V. Jones, P. Mahanti, K. P. Chen, T. J. Taylor and M. A. Hayes, Dielectrophoretic mobility determination in DC insulator-based dielectrophoresis, *Electrophoresis*, 2011, **32**(17), 2292–2297.
128 A. Nakano, T. C. Chao, F. Camacho-Alanis and A. Ros, Immunoglobulin G and bovine serum albumin streaming dielectrophoresis in a microfluidic device, *Electrophoresis*, 2011, **32**(17), 2314–2322.
129 Y. Liu, A. Jiang, E. Kim, C. Ro, T. Adams, L. A. Flanagan, T. J. Taylor and M. A. Hayes, Identification of neural stem and progenitor cell subpopulations using DC insulator-based dielectrophoresis, *Analyst*, 2019, **144**(13), 4066–4072.
130 A. Salmanzadeh, L. Romero, H. Shafiee, R. C. Gallo-Villanueva, M. A. Stremler, S. D. Cramer and R. V. Davalos, Isolation of prostate tumor initiating cells (TICs) through their dielectrophoretic signature, *Lab Chip*, 2012, **12**(1), 182–189.
131 C. Hanson, J. T. Barney, M. M. Bishop and E. Vargis, Simultaneous isolation and label-free identification of bacteria using contactless dielectrophoresis and Raman spectroscopy, *Electrophoresis*, 2019, **40**(10), 1446–1456.
132 H. Shafiee, M. B. Sano, E. A. Henslee, J. L. Caldwell and R. V. Davalos, Selective isolation of live/dead cells using contactless dielectrophoresis (cDEP), *Lab Chip*, 2010, **10**(4), 438–445.

133 P. Puri, V. Kumar, S. Belgamwar and N. Sharma, Microfluidic device for cell trapping with carbon electrodes using dielectrophoresis, *Biomed. Microdevices*, 2018, **20**, 1–10.

134 N. N. Mohd Maidin, M. R. Buyong, R. A. Rahim and M. A. Mohamed, Dielectrophoresis applications in biomedical field and future perspectives in biomedical technology, *Electrophoresis*, 2021, **42**(20), 2033–2059.

135 C. Hanson, M. Sieverts, K. Tew, A. Dykes, M. Salisbury and E. Vargis, The use of microfluidics and dielectrophoresis for separation, concentration, and identification of bacteria, in *Microfluidics, BioMEMS, and Medical Microsystems XIV*, SPIE, 2016, pp 65–73.

136 A. Rahmani, A. Mohammadi and H. R. Kalhor, A continuous flow microfluidic device based on contactless dielectrophoresis for bioparticles enrichment, *Electrophoresis*, 2018, **39**(3), 445–455.

137 A. Kale, A. Malekanfard and X. Xuan, Analytical Guidelines for Designing Curvature-Induced Dielectrophoretic Particle Manipulation Systems, *Micromachines*, 2020, **11**(7), 707.

138 J. Zhu and X. Xuan, Curvature-induced dielectrophoresis for continuous separation of particles by charge in spiral microchannels, *Biomicrofluidics*, 2011, **5**(2), 024111.

139 P. V. Jones and M. A. Hayes, Development of the resolution theory for gradient insulator-based dielectrophoresis, *Electrophoresis*, 2015, **36**(9–10), 1098–1106.

140 J. Ding, R. M. Lawrence, P. V. Jones, B. G. Hogue and M. A. Hayes, Concentration of Sindbis virus with optimized gradient insulator-based dielectrophoresis, *Analyst*, 2016, **141**(6), 1997–2008.

141 W. M. Arnold, Positioning and levitation media for the separation of biological cells, *IEEE Trans. Ind. Appl.*, 2001, **37**(5), 1468–1475.

142 M. Li, S. Li, W. Cao, W. Li, W. Wen and G. Alici, Improved concentration and separation of particles in a 3D dielectrophoretic chip integrating focusing, aligning and trapping, *Microfluid. Nanofluid.*, 2013, **14**(3), 527–539.

143 M. Muratore, V. Srsen, M. Waterfall, A. Downes and R. Pethig, Biomarker-free dielectrophoretic sorting of differentiating myoblast multipotent progenitor cells and their membrane analysis by Raman spectroscopy, *Biomicrofluidics*, 2012, **6**(3), 034113.

144 F. Alnaimat, B. Mathew and A. Hilal-Alnaqbi, Modeling a Dielectrophoretic Microfluidic Device with Vertical Interdigitated Transducer Electrodes for Separation of Microparticles Based on Size, *Micromachines*, 2020, **11**(6), 563.

145 N. Lewpiriyawong, C. Yang and Y. C. Lam, Continuous sorting and separation of microparticles by size using AC dielectrophoresis in a PDMS microfluidic device with 3-D conducting PDMS composite electrodes, *Electrophoresis*, 2010, **31**(15), 2622–2631.

146 I. F. Cheng, V. E. Froude, Y. Zhu, H.-C. Chang and H.-C. Chang, A continuous high-throughput bioparticle sorter based on 3D traveling-wave dielectrophoresis, *Lab Chip*, 2009, **9**(22), 3193–3201.

147 H. Song, J. M. Rosano, Y. Wang, C. J. Garson, B. Prabhakarpandian, K. Pant, G. J. Klarmann, A. Perantoni, L. M. Alvarez and E. Lai, Continuous-flow sorting of stem cells and differentiation products based on dielectrophoresis, *Lab Chip*, 2015, **15**(5), 1320–1328.

148 X. Huang, K. Torres-Castro, W. Varhue, A. Salahi, A. Rasin, C. Honrado, A. Brown, J. Guler and N. S. Swami, Self-aligned sequential lateral field non-uniformities over channel depth for high throughput dielectrophoretic cell deflection, *Lab Chip*, 2021, **21**(5), 835–843.

149 M. Olfat and E. Kadivar, Particle separation based on dielectrophoresis force using boundary element method and point-particle approach in a microfluidic channel, *Microfluid. Nanofluid.*, 2023, **27**(12), 83.

150 A. Sonnenberg, J. Y. Marciniak, J. McCanna, R. Krishnan, L. Rassenti, T. J. Kipps and M. J. Heller, Dielectrophoretic isolation and detection of cfc-DNA nanoparticulate biomarkers and virus from blood, *Electrophoresis*, 2013, **34**(7), 1076–1084.

151 S. Ibsen, A. Sonnenberg, C. Schutt, R. Mukthavaram, Y. Yeh, I. Ortac, S. Manouchehri, S. Kesari, S. Esener and M. J. Heller, Recovery of drug delivery nanoparticles from human plasma using an electrokinetic platform technology, *Small*, 2015, **11**(38), 5088–5096.

152 C. Yu, J. Vykoukal, D. M. Vykoukal, J. A. Schwartz, L. Shi and P. R. Gascoyne, A three-dimensional dielectrophoretic particle focusing channel for microcytometry applications, *J. Microelectromech. Syst.*, 2005, **14**(3), 480–487.

153 J. P. Beech, P. Jönsson and J. O. Tegenfeldt, Tipping the balance of deterministic lateral displacement devices using dielectrophoresis, *Lab Chip*, 2009, **9**(18), 2698–2706.

154 T. Yasukawa, M. Suzuki, T. Sekiya, H. Shiku and T. Matsue, Flow sandwich-type immunoassay in microfluidic devices based on negative dielectrophoresis, *Biosens. Bioelectron.*, 2007, **22**(11), 2730–2736.

155 S. Burgarella, S. Merlo, B. Dell'Anna, G. Zarola and M. Bianchessi, A modular micro-fluidic platform for cells handling by dielectrophoresis, *Microelectron. Eng.*, 2010, **87**(11), 2124–2133.

156 Y. Ai and S. Qian, DC dielectrophoretic particle–particle interactions and their relative motions, *J. Colloid Interface Sci.*, 2010, **346**(2), 448–454.

157 Z. Gagnon, J. Mazur and H.-C. Chang, Integrated AC electrokinetic cell separation in a closed-loop device, *Lab Chip*, 2010, **10**(6), 718–726.

158 H. Maruyama, K. Kotani, T. Masuda, A. Honda, T. Takahata and F. Arai, Nanomanipulation of single influenza virus using dielectrophoretic concentration and optical tweezers for single virus infection to a specific cell on a microfluidic chip, *Microfluid. Nanofluid.*, 2011, **10**, 1109–1117.

159 J. Fathy, A. Pourmand and H. B. Ghavifekr, Design and simulation of a MEMS based cell separator utilizing 3D travelling-wave dielectrophoresis, *Microsyst. Technol.*, 2017, **23**(5), 1351–1360.

160 M. Farasat, E. Aalaei, S. Kheirati Ronizi, A. Bakhshi, S. Mirhosseini, J. Zhang, N.-T. Nguyen and N. Kashaninejad, Signal-Based Methods in Dielectrophoresis for Cell and Particle Separation, *Biosensors*, 2022, **12**(7), 510.

161 B. H. Lapizco-Encinas and M. Rito-Palomares, Dielectrophoresis for the manipulation of nanobioparticles, *Electrophoresis*, 2007, **28**(24), 4521–4538.

162 M. Kumemura, D. Collard, C. Yamahata, N. Sakaki, G. Hashiguchi and H. Fujita, Single DNA molecule isolation and trapping in a microfluidic device, *ChemPhysChem*, 2007, **8**(12), 1875–1880.

163 C.-P. Jen, H.-H. Chang, C.-T. Huang and K.-H. Chen, A microfabricated module for isolating cervical carcinoma cells from peripheral blood utilizing dielectrophoresis in stepping electric fields, *Microsyst. Technol.*, 2012, **18**(11), 1887–1896.

164 M. A. Md Ali, K. Ostrikov, F. A. Khalid, B. Y. Majlis and A. A. Kayani, Active bioparticle manipulation in microfluidic systems, *RSC Adv.*, 2016, **6**(114), 113066–113094.

165 A. Morimoto, T. Mogami, M. Watanabe, K. Iijima, Y. Akiyama, K. Katayama, T. Futami, N. Yamamoto, T. Sawada, F. Koizumi and Y. Koh, High-Density Dielectrophoretic Microwell Array for Detection, Capture, and Single-Cell Analysis of Rare Tumor Cells in Peripheral Blood, *PLoS One*, 2015, **10**(6), e0130418.

166 C.-F. Chou, J. O. Tegenfeldt, O. Bakajin, S. S. Chan, E. C. Cox, N. Darnton, T. Duke and R. H. Austin, Electrodeless dielectrophoresis of single-and double-stranded DNA, *Biophys. J.*, 2002, **83**(4), 2170–2179.

167 R. C. Gallo-Villanueva, C. E. Rodríguez-López, R. I. Díaz-de-la-Garza, C. Reyes-Betanzo and B. H. Lapizco-Encinas, DNA manipulation by means of insulator-based dielectrophoresis employing direct current electric fields, *Electrophoresis*, 2009, **30**(24), 4195–4205.

168 P. B. Bareil, Y. Sheng, Y.-Q. Chen and A. Chiou, Calculation of spherical red blood cell deformation in a dual-beam optical stretcher, *Opt. Express*, 2007, **15**(24), 16029–16034.

169 P.-H. Wu, D. R.-B. Aroush, A. Asnacios, W.-C. Chen, M. E. Dokukin, B. L. Doss, P. Durand-Smet, A. Ekpenyong, J. Guck and N. V. Guz, A comparison of methods to assess cell mechanical properties, *Nat. Methods*, 2018, **15**(7), 491–498.

170 E. Zhou, F. Xu, S. Quek and C. Lim, A power-law rheology-based finite element model for single cell deformation, *Biomech. Model. Mechanobiol.*, 2012, **11**, 1075–1084.

171 H. Bow, I. V. Pivkin, M. Diez-Silva, S. J. Goldfless, M. Dao, J. C. Niles, S. Suresh and J. Han, A microfabricated deformability-based flow cytometer with application to malaria, *Lab Chip*, 2011, **11**(6), 1065–1073.

172 A. Valero, T. Braschler and P. Renaud, A unified approach to dielectric single cell analysis: Impedance and dielectrophoretic force spectroscopy, *Lab Chip*, 2010, **10**(17), 2216–2225.

173 D. Krinke, H.-G. Jahnke, O. Pänke and A. A. Robitzki, A microelectrode-based sensor for label-free *in vitro* detection of ischemic effects on cardiomyocytes, *Biosens. Bioelectron.*, 2009, **24**(9), 2798–2803.

174 Y. Feng, L. Huang, P. Zhao, F. Liang and W. Wang, A microfluidic device integrating impedance flow cytometry and electric impedance spectroscopy for high-efficiency single-cell electrical property measurement, *Anal. Chem.*, 2019, **91**(23), 15204–15212.

175 Y. Seki, A. Nagasaka, T. Gondo and S. Tada, Proposal and performance evaluation of a new parallel plate continuous cell separation device using dielectrophoresis, *Electrophoresis*, 2024, **45**, 1673–1683.

176 S. L. Stott, C.-H. Hsu, D. I. Tsukrov, M. Yu, D. T. Miyamoto, B. A. Waltman, S. M. Rothenberg, A. M. Shah, M. E. Smas and G. K. Korir, Isolation of circulating tumor cells using a microvortex-generating herringbone-chip, *Proc. Natl. Acad. Sci. U. S. A.*, 2010, **107**(43), 18392–18397.

177 G. M. Whitesides, The origins and the future of microfluidics, *nature*, 2006, **442**(7101), 368–373.

178 M. Alshareef, N. Metrakos, E. Juarez Perez, F. Azer, F. Yang, X. Yang and G. Wang, Separation of tumor cells with dielectrophoresis-based microfluidic chip, *Biomicrofluidics*, 2013, **7**(1), 11803.

179 Z. Çağlayan, Y. Demircan Yalçın and H. Külah, Examination of the dielectrophoretic spectra of MCF7 breast cancer cells and leukocytes, *Electrophoresis*, 2020, **41**(5–6), 345–352.

180 F. Yang, X. Yang, H. Jiang, P. Bulkhaults, P. Wood, W. Hrushesky and G. Wang, Dielectrophoretic separation of colorectal cancer cells, *Biomicrofluidics*, 2010, **4**(1), 13204.

181 L. A. Flanagan, J. Lu, L. Wang, S. A. Marchenko, N. L. Jeon, A. P. Lee and E. S. Monuki, Unique dielectric properties distinguish stem cells and their differentiated progeny, *Stem Cell.*, 2008, **26**(3), 656–665.

182 A. Salari, M. Navi and C. Dalton, A novel alternating current multiple array electrothermal micropump for lab-on-a-chip applications, *Biomicrofluidics*, 2015, **9**(1), 014113.

183 J. Kadaksham, P. Singh and N. Aubry, Dielectrophoresis induced clustering regimes of viable yeast cells, *Electrophoresis*, 2005, **26**(19), 3738–3744.

184 N. Manaresi, A. Romani, G. Medoro, L. Altomare, A. Leonardi, M. Tartagni and R. Guerrieri, A CMOS chip for individual cell manipulation and detection, *IEEE J. Solid State Circ.*, 2003, **38**(12), 2297–2305.

185 M. P. Hughes, H. Morgan and F. J. Rixon, Measuring the dielectric properties of herpes simplex virus type 1 virions with dielectrophoresis, *Biochim. Biophys. Acta, Gen. Subj.*, 2002, **1571**(1), 1–8.

186 H. Morgan and N. G. Green, *AC Electrokinetics: Colloids and Nanoparticles*, Research Studies Press, 2003.

187 M. Mita, H. Kawara, H. Toshiyoshi, J. Endo and H. Fujita, Bulk micromachined tunneling tips integrated with positioning actuators, *J. Microelectromech. Syst.*, 2005, **14**(1), 23–28.

188 P. R. Gascoyne and J. V. Vykoukal, Dielectrophoresis-based sample handling in general-purpose programmable diagnostic instruments, *Proc. IEEE*, 2004, **92**(1), 22–42.
189 D. Chatterjee, B. Hetayothin, A. R. Wheeler, D. J. King and R. L. Garrell, Droplet-based microfluidics with nonaqueous solvents and solutions, *Lab Chip*, 2006, **6**(2), 199–206.
190 M. R. Hossan, D. Dutta, N. Islam and P. Dutta, Review: Electric field driven pumping in microfluidic device, *Electrophoresis*, 2018, **39**(5–6), 702–731.
191 D. Sun and K. Böhringer, Self-Cleaning: From Bio-Inspired Surface Modification to MEMS/Microfluidics System Integration, *Micromachines*, 2019, **10**, 101.
192 J. Lee, H. Moon, J. Fowler, T. Schoellhammer and C.-J. Kim, Electrowetting and electrowetting-on-dielectric for microscale liquid handling, *Sens. Actuators, A*, 2002, **95**(2–3), 259–268.
193 S. Zeng, C.-H. Chen, J. C. Mikkelsen and J. G. Santiago, Fabrication and characterization of electroosmotic micropumps, *Sens. Actuators, B*, 2001, **79**(2), 107–114.
194 M. Gao and L. Gui, Development of a Multi-Stage Electroosmotic Flow Pump Using Liquid Metal Electrodes, *Micromachines*, 2016, **7**(9), 165.
195 O. D. Velev and K. H. Bhatt, On-chip micromanipulation and assembly of colloidal particles by electric fields, *Soft Matter*, 2006, **2**(9), 738–750.
196 W.-L. Hsu, D. W. Inglis, M. A. Startsev, E. M. Goldys, M. R. Davidson and D. J. E. Harvie, Isoelectric Focusing in a Silica Nanofluidic Channel: Effects of Electromigration and Electroosmosis, *Anal. Chem.*, 2014, **86**(17), 8711–8718.
197 A. Alizadeh, W. L. Hsu, M. Wang and H. Daiguji, Electroosmotic flow: From microfluidics to nanofluidics, *Electrophoresis*, 2021, **42**(7–8), 834–868.
198 A. González, A. Ramos, N. G. Green, A. Castellanos and H. Morgan, Fluid flow induced by nonuniform ac electric fields in electrolytes on microelectrodes. II. A linear double-layer analysis, *Phys. Rev. E: Stat. Phys., Plasmas, Fluids, Relat. Interdiscip. Top.*, 2000, **61**(4), 4019.
199 S.-J. Liu, H.-H. Wei, S.-H. Hwang and H.-C. Chang, Dynamic particle trapping, release, and sorting by microvortices on a substrate, *Phys. Rev. E: Stat., Nonlinear, Soft Matter Phys.*, 2010, **82**(2), 026308.
200 H. Zhou, L. R. White and R. D. Tilton, Lateral separation of colloids or cells by dielectrophoresis augmented by AC electroosmosis, *J. Colloid Interface Sci.*, 2005, **285**(1), 179–191.
201 J. Wu, Y. Ben, D. Battigelli and H.-C. Chang, Long-Range AC Electroosmotic Trapping and Detection of Bioparticles, *Ind. Eng. Chem. Res.*, 2005, **44**(8), 2815–2822.
202 G. Tang, D. Yan, C. Yang, H. Gong, J. C. Chai and Y. C. Lam, Assessment of Joule heating and its effects on electroosmotic flow and electrophoretic transport of solutes in microfluidic channels, *Electrophoresis*, 2006, **27**(3), 628–639.
203 S. V. Puttaswamy, S. Sivashankar, C.-H. Yeh, R.-J. Chen and C. H. Liu, Electrodynamically actuated on-chip flow cytometry with low shear stress for electro-osmosis based sorting using low conductive medium, *Microelectron. Eng.*, 2010, **87**(12), 2582–2591.
204 G. Beni and S. Hackwood, Electro-wetting displays, *Appl. Phys. Lett.*, 1981, **38**(4), 207–209.
205 J. Lee and C.-J. Kim, Surface-tension-driven microactuation based on continuous electrowetting, *J. Microelectromech. Syst.*, 2000, **9**(2), 171–180.
206 H.-H. Shen, S.-K. Fan, C.-J. Kim and D.-J. Yao, EWOD microfluidic systems for biomedical applications, *Microfluid. Nanofluid.*, 2014, **16**, 965–987.
207 M. G. Pollack, A. D. Shenderov and R. B. Fair, Electrowetting-based actuation of droplets for integrated microfluidics, *Lab Chip*, 2002, **2**(2), 96–101.
208 C. Sung Kwon, M. Hyejin and K. Chang-Jin, Creating, transporting, cutting, and merging liquid droplets by electrowetting-based actuation for digital microfluidic circuits, *J. Microelectromech. Syst.*, 2003, **12**(1), 70–80.
209 Y. Zhao, U. C. Yi and S. K. Cho, Microparticle Concentration and Separation by Traveling-Wave Dielectrophoresis (twDEP) for Digital Microfluidics, *J. Microelectromech. Syst.*, 2007, **16**(6), 1472–1481.
210 M. G. Pollack, R. B. Fair and A. D. Shenderov, Electrowetting-based actuation of liquid droplets for microfluidic applications, *Appl. Phys. Lett.*, 2000, **77**(11), 1725–1726.
211 V. Srinivasan, V. K. Pamula and R. B. Fair, An integrated digital microfluidic lab-on-a-chip for clinical diagnostics on human physiological fluids, *Lab Chip*, 2004, **4**(4), 310–315.
212 I. Barbulovic-Nad, H. Yang, P. S. Park and A. R. Wheeler, Digital microfluidics for cell-based assays, *Lab Chip*, 2008, **8**(4), 519–526.
213 L. K. Minor, Label-free cell-based functional assays, *Comb. Chem. High Throughput Screening*, 2008, **11**(7), 573–580.
214 A. B. Theberge, F. Courtois, Y. Schaerli, M. Fischlechner, C. Abell, F. Hollfelder and W. T. S. Huck, Microdroplets in Microfluidics: An Evolving Platform for Discoveries in Chemistry and Biology, *Angew. Chem., Int. Ed.*, 2010, **49**(34), 5846–5868.
215 H. Hufnagel, A. Huebner, C. Gülch, K. Güse, C. Abell and F. Hollfelder, An integrated cell culture lab on a chip: modular microdevices for cultivation of mammalian cells and delivery into microfluidic microdroplets, *Lab Chip*, 2009, **9**(11), 1576–1582.
216 Z. Yu, J. Jin, S. Chen, L. Shui, H. Chen, L. Shi and Y. Zhu, Smart Droplet Microfluidic System for Single-Cell Selective Lysis and Real-Time Sorting Based on Microinjection and Image Recognition, *Anal. Chem.*, 2023, **95**(34), 12875–12883.
217 S. Paul and H. Moon, Drop-to-drop liquid–liquid extraction of DNA in an electrowetting-on-dielectric digital microfluidics, *Biomicrofluidics*, 2021, **15**(3), 034110.
218 R. Shen, S. Yi, P. Wang, P.-I. Mak, R. P. Martins and Y. Jia, Nucleic acid analysis on electrowetting-based digital microfluidics, *Trac. Trends Anal. Chem.*, 2023, **158**, 116826.
219 S. Kalsi, M. Valiadi, C. Turner, M. Sutton and H. Morgan, Sample pre-concentration on a digital microfluidic

platform for rapid AMR detection in urine, *Lab Chip*, 2019, **19**(1), 168–177.

220 G. Karapetsas, K. C. Sahu, K. Sefiane and O. K. Matar, Thermocapillary-driven motion of a sessile drop: effect of non-monotonic dependence of surface tension on temperature, *Langmuir*, 2014, **30**(15), 4310–4321.

221 T. K. Jun and C.-J. C. Kim, Valveless pumping using traversing vapor bubbles in microchannels, *J. Appl. Phys.*, 1998, **83**(11), 5658–5664.

222 Y. Katagiri, Optical micromachines for photonic networks, in *Optomechatronic Systems II*, SPIE, 2001, pp 152–163.

223 S.-K. Fan, H. Yang, T.-T. Wang and W. Hsu, Asymmetric electrowetting—Moving droplets by a square wave, *Lab Chip*, 2007, **7**(10), 1330–1335.

224 L.-H. Chau, W. Liang, F. W. K. Cheung, W. K. Liu, W. J. Li, S.-C. Chen and G.-B. Lee, Self-Rotation of Cells in an Irrotational AC E-Field in an Opto-Electrokinetics Chip, *PLoS One*, 2013, **8**(1), e51577.

225 M. Ouyang, W. Ki Cheung, W. Liang, J. D. Mai, W. Keung Liu and W. Jung Li, Inducing self-rotation of cells with natural and artificial melanin in a linearly polarized alternating current electric field, *Biomicrofluidics*, 2013, **7**(5), 54112.

226 M. P. Hughes, S. Archer and H. Morgan, Mapping the electrorotational torque in planar microelectrodes, *J. Phys. D: Appl. Phys.*, 1999, **32**(13), 1548.

227 C. Huang, A. Chen, M. Guo and J. Yu, Membrane dielectric responses of bufalin-induced apoptosis in HL-60 cells detected by an electrorotation chip, *Biotechnol. Lett.*, 2007, **29**(9), 1307–1313.

228 C. F. Wilson, M. I. Wallace, K. Morishima, G. J. Simpson and R. N. Zare, Coupled electrorotation of polymer microspheres for microfluidic sensing and mixing, *Anal. Chem.*, 2002, **74**(19), 5099–5104.

229 S.-I. Han, Y.-D. Joo and K.-H. Han, An electrorotation technique for measuring the dielectric properties of cells with simultaneous use of negative quadrupolar dielectrophoresis and electrorotation, *Analyst*, 2013, **138**(5), 1529–1537.

230 J. L. Prieto, H.-W. Su, H. W. Hou, M. P. Vera, B. D. Levy, R. M. Baron, J. Han and J. Voldman, Monitoring sepsis using electrical cell profiling, *Lab Chip*, 2016, **16**(22), 4333–4340.

231 K. Cheung, S. Gawad and P. Renaud, Impedance spectroscopy flow cytometry: On-chip label-free cell differentiation, *Cytometry, Part A*, 2005, **65**(2), 124–132.

232 W.-H. Huang, F. Ai, Z.-L. Wang and J.-K. Cheng, Recent advances in single-cell analysis using capillary electrophoresis and microfluidic devices, *J. Chromatogr. B*, 2008, **866**(1), 104–122.

233 Y. Liu, H. Wang, J. Lu, Y. Miao, X. Cao, L. Zhang, X. Wu, F. Wu, B. Ding, R. Wang, M. Luo, W. Li and J. Tan, Rex Rabbit Somatic Cell Nuclear Transfer with In Vitro-Matured Oocytes, *Cell. Reprogram.*, 2016, **18**(3), 187–194.

234 U. Lei, P.-H. Sun and R. Pethig, Refinement of the theory for extracting cell dielectric properties from dielectrophoresis and electrorotation experiments, *Biomicrofluidics*, 2011, **5**(4), 44109.

235 M. Habaza, M. Kirschbaum, C. Guernth-Marschner, G. Dardikman, I. Barnea, R. Korenstein, C. Duschl and N. T. Shaked, Rapid 3D refractive-index imaging of live cells in suspension without labeling using dielectrophoretic cell rotation, *Adv. Sci.*, 2017, **4**(2), 1600205.

236 A. Adamo, O. Roushdy, R. Dokov, A. Sharei and K. Jensen, Microfluidic jet injection for delivering macromolecules into cells, *J. Micromech. Microeng.*, 2013, **23**(3), 035026.

237 K. Keim, M. Z. Rashed, S. C. Kilchenmann, A. Delattre, A. F. Gonçalves, P. Éry and C. Guiducci, On-chip technology for single-cell arraying, electrorotation-based analysis and selective release, *Electrophoresis*, 2019, **40**(14), 1830–1838.

238 C. Trainito, O. Français and B. Le Pioufle, A microfluidic device to determine dielectric properties of a single cell: a combined dielectrophoresis and electrorotation technique, in *4th European Conference on Microfluidics*, 2014.

239 G. Bahrieh, M. Erdem, E. Özgür, U. Gündüz and H. Külah, Assessment of effects of multi drug resistance on dielectric properties of K562 leukemic cells using electrorotation, *RSC Adv.*, 2014, **4**(85), 44879–44887.

240 L. Huang, F. Liang, P. Zhao, Y. Feng, W. He and W. Wang, A microfluidic chip combining optical stretcher and electro-rotation for measuring cellular mechanical and electrical properties, in *22nd International Conference on Miniaturized Systems for Chemistry and Life Sciences*, Kaohsiung, Taiwan, 2018, pp. 1367–1369.

241 L. Huang, F. Liang, Y. Feng, P. Zhao and W. Wang, On-chip integrated optical stretching and electrorotation enabling single-cell biophysical analysis, *Microsyst. Nanoeng.*, 2020, **6**(1), 57.

242 L. Huang, P. Zhao and W. Wang, 3D cell electrorotation and imaging for measuring multiple cellular biophysical properties, *Lab Chip*, 2018, **18**(16), 2359–2368.

243 C. Trainito, E. Bayart, F. Subra, O. Français and B. Le Pioufle, The electrorotation as a tool to monitor the dielectric properties of spheroid during the permeabilization, *J. Membr. Biol.*, 2016, **249**, 593–600.

244 C. Vaillier, T. Honegger, F. Kermarrec, X. Gidrol and D. Peyrade, Comprehensive analysis of human cells motion under an irrotational AC electric field in an electro-microfluidic chip, *PLoS One*, 2014, **9**(4), e95231.

245 L. Huang, F. Liang and Y. Feng, A microfluidic chip for single-cell 3D rotation enabling self-adaptive spatial localization, *J. Appl. Phys.*, 2019, **126**(23), 234702.

246 C. I. Trainito, O. Français and B. Le Pioufle, Monitoring the permeabilization of a single cell in a microfluidic device, through the estimation of its dielectric properties based on combined dielectrophoresis and electrorotation *in situ* experiments, *Electrophoresis*, 2015, **36**(9–10), 1115–1122.

247 L. Huang, W. He and W. Wang, A cell electro-rotation micro-device using polarized cells as electrodes, *Electrophoresis*, 2019, **40**(5), 784–791.

248 S. Kilchenmann, *Microfluidic and Electrokinetic Manipulation of Single Cells*, EPFL, 2017.
249 W. Liu, Y. Ren, Y. Tao, Y. Li and X. Chen, Controllable rotating behavior of individual dielectric microrod in a rotating electric field, *Electrophoresis*, 2017, **38**(11), 1427–1433.
250 P. Benhal, G. Chase, P. Gaynor, B. Oback and W. Wang, Multiple-cylindrical electrode system for rotational electric field generation in particle rotation applications, *Int. J. Adv. Rob. Syst.*, 2015, **12**(7), 84.
251 L. Huang, L. Tu, X. Zeng, L. Mi, X. Li and W. Wang, Study of a microfluidic chip integrating single cell trap and 3D stable rotation manipulation, *Micromachines*, 2016, **7**(8), 141.
252 W. Liang, K. Zhang, X. Yang, L. Liu, H. Yu and W. Zhang, Distinctive translational and self-rotational motion of lymphoma cells in an optically induced non-rotational alternating current electric field, *Biomicrofluidics*, 2015, **9**(1), 014121.
253 M. Annabestani, H. Mohammadzadeh, A. Aghassizadeh, S. Azizmohseni and M. Fardmanesh, Active Microfluidic Micromixer Design using Ionic Polymer-Metal Composites, in *27th Iranian Conference on Electrical Engineering (ICEE)*, 2019, pp 371–375.
254 B. Zhao, X. Cui, W. Ren, F. Xu, M. Liu and Z.-G. Ye, A Controllable and Integrated Pump-enabled Microfluidic Chip and Its Application in Droplets Generating, *Sci. Rep.*, 2017, **7**(1), 11319.
255 S.-K. Fan, T.-H. Hsieh and D.-Y. Lin, General digital microfluidic platform manipulating dielectric and conductive droplets by dielectrophoresis and electrowetting, *Lab Chip*, 2009, **9**(9), 1236–1242.
256 X. Wang, C. Cheng, S. Wang and S. Liu, Electroosmotic pumps and their applications in microfluidic systems, *Microfluid. Nanofluid.*, 2009, **6**(2), 145–162.
257 P.-W. Yen, S.-C. Lin, Y.-C. Huang, Y.-J. Huang, Y.-C. Tung, S.-S. Lu and C.-T. Lin, A Low-Power CMOS Microfluidic Pump Based on Travelling-Wave Electroosmosis for Diluted Serum Pumping, *Sci. Rep.*, 2019, **9**(1), 14794.
258 J. W. Munyan, H. V. Fuentes, M. Draper, R. T. Kelly and A. T. Woolley, Electrically actuated, pressure-driven microfluidic pumps, *Lab Chip*, 2003, **3**(4), 217–220.
259 M. Ghodbane, E. C. Stucky, T. J. Maguire, R. S. Schloss, D. I. Shreiber, J. D. Zahn and M. L. Yarmush, Development and validation of a microfluidic immunoassay capable of multiplexing parallel samples in microliter volumes, *Lab Chip*, 2015, **15**(15), 3211–3221.
260 W. Jung, J. Han, J.-W. Choi and C. H. Ahn, Point-of-care testing (POCT) diagnostic systems using microfluidic lab-on-a-chip technologies, *Microelectron. Eng.*, 2015, **132**, 46–57.
261 C.-Y. Lee, C.-L. Chang, Y.-N. Wang and L.-M. Fu, Microfluidic Mixing: A Review, *Int. J. Mol. Sci.*, 2011, **12**(5), 3263–3287.
262 N. Y. Lee, M. Yamada and M. Seki, Pressure-driven sample injection with quantitative liquid dispensing for on-chip electrophoresis, *Anal. Sci.*, 2004, **20**(3), 483–487.
263 E. M. Smith, H. Xu and A. G. Ewing, DNA separations in microfabricated devices with automated capillary sample introduction, *Electrophoresis*, 2001, **22**(2), 363–370.
264 A. Abou-Hassan, O. Sandre and V. Cabuil, Microfluidics in Inorganic Chemistry, *Angew. Chem., Int. Ed.*, 2010, **49**(36), 6268–6286.
265 S. E. Chung, S. A. Lee, J. Kim and S. Kwon, Optofluidic encapsulation and manipulation of silicon microchips using image processing based optofluidic maskless lithography and railed microfluidics, *Lab Chip*, 2009, **9**(19), 2845–2850.
266 K. Ren, J. Zhou and H. Wu, Materials for Microfluidic Chip Fabrication, *Acc. Chem. Res.*, 2013, **46**(11), 2396–2406.
267 X. Hou, Y. S. Zhang, G. T.-d. Santiago, M. M. Alvarez, J. Ribas, S. J. Jonas, P. S. Weiss, A. M. Andrews, J. Aizenberg and A. Khademhosseini, Interplay between materials and microfluidics, *Nat. Rev. Mater.*, 2017, **2**(5), 17016.
268 A. C. Henry, T. J. Tutt, M. Galloway, Y. Y. Davidson, C. S. McWhorter, S. A. Soper and R. L. McCarley, Surface Modification of Poly(methyl methacrylate) Used in the Fabrication of Microanalytical Devices, *Anal. Chem.*, 2000, **72**(21), 5331–5337.
269 S. L. R. Barker, D. Ross, M. J. Tarlov, M. Gaitan and L. E. Locascio, Control of Flow Direction in Microfluidic Devices with Polyelectrolyte Multilayers, *Anal. Chem.*, 2000, **72**(24), 5925–5929.
270 J. S. Rossier, G. Gokulrangan, H. H. Girault, S. Svojanovsky and G. S. Wilson, Characterization of Protein Adsorption and Immunosorption Kinetics in Photoablated Polymer Microchannels, *Langmuir*, 2000, **16**(22), 8489–8494.
271 H. Tang, J. Niu, H. Jin, S. Lin and D. Cui, Geometric structure design of passive label-free microfluidic systems for biological micro-object separation, *Microsyst. Nanoeng.*, 2022, **8**(1), 62.
272 F. Wang, S. Lin, Z. Yu, Y. Wang, D. Zhang, C. Cao, Z. Wang, D. Cui and D. Chen, Recent advances in microfluidic-based electroporation techniques for cell membranes, *Lab Chip*, 2022, **22**(14), 2624–2646.
273 T. Lan, D. Cui, T. Liu, X. Yu and M. Huang, Gold NanoStars: Synthesis, Modification and Application, *Nano Biomed. Eng.*, 2023, **15**(3), 330–341.
274 J. Niu, S. Lin, D. Chen, Z. Wang, C. Cao, A. Gao, S. Cui, Y. Liu, Y. Hong and X. Zhi, A Fully Elastic Wearable Electrochemical Sweat Detection System of Tree-Bionic Microfluidic Structure for Real-Time Monitoring, *Small*, 2024, **20**(11), 2306769.
275 X. Zhi, M. Deng, H. Yang, G. Gao, K. Wang, H. Fu, Y. Zhang, D. Chen and D. Cui, A novel HBV genotypes detecting system combined with microfluidic chip, loop-mediated isothermal amplification and GMR sensors, *Biosens. Bioelectron.*, 2014, **54**, 372–377.
276 Y. Xie, X. Zhi, H. Su, K. Wang, Z. Yan, N. He, J. Zhang, D. Chen and D. Cui, A Novel Electrochemical Microfluidic Chip Combined with Multiple Biomarkers for Early Diagnosis of Gastric Cancer, *Nanoscale Res. Lett.*, 2015, **10**(1), 477.